UNIVERSITÀ DEGLI STUDI DI UDINE

Dipartimento di Scienze e Tecnologie Biomediche

Tesi di Dottorato in Scienze Biomediche e Biotecnologiche

XXVI CICLO

Role of p27kip1 in the regulation of miR-223 following contact inhibition

Relatore

Dott. Gustavo Baldassarre

Correlatrice

Dott.ssa Barbara Belletti

Coordinatore

Prof. Claudio Brancolini

Dottorando

Dott. Joshua Armenia

Anno Accademico 2013/2014

TABLE OF CONTENTS

Abstract

microRNAs (also called miRs or miRNAs) are a large class of small regulatory RNAs that function as nodes of signaling networks. This implicates that miRs expression has to be finely tuned, as observed during cell cycle progression. Using an expression profiling approach, we provide evidence that the CDK inhibitor p27kip1 regulates miRs expression following cell cycle exit. By using wild type and p27KO cells, harvested in different phases of the cell cycle, we identified several miRs regulated by p27kip1 during the G1 to S phase transition. Among these miRs, miR-223 was a miR specifically upregulated by p27kip1 in G1 arrested cells. During the work of this PhD thesis, we demonstrated that p27kip1 regulates the expression of miR-223, via two distinct mechanisms. First, p27kip1 directly stabilized mature miR-223 expression, acting as a RNA binding protein. Second, p27kip1 controlled E2F1 expression that, in turn, regulated miR-223 promoter activity. The resulting elevated miR-223 levels ultimately participated to cell cycle arrest following contact inhibition.

Introduction

1 microRNA

The first evidence of the existence of microRNAs (also called miRs or miRNAs) came from the discovery of a 22-nucleotide non-coding RNA (lin-4) partially complementary to 7 conserved sites located in the 3′-untranslated region (3'-UTR) of the lin-14 gene (1, 2). Strikingly, the negative regulation of lin-14 protein expression required an intact 3′-UTR of its mRNA, as well as a functional lin-4 gene (1, 2). It was reported that lin-4 and let-7, the first miR genes identified, control developmental timing in nematodes by modulating the expression of other genes at the post-transcriptional level (1, 2, 3).

miRs are a class of 20–25 nucleotide-long noncoding RNAs that modulate gene expression through canonical base pairing between the seed sequence of the miR (nucleotides 2–8 at its 5′ end) and its complementary seed match sequence (which is present in the 3′ UTR of target mRNAs) (4).

Current estimates suggest that the human genome contains at least hundreds of distinct miRs, which potentially regulate a large fraction of the transcriptome and are potentially involved in any phisiological and pathological condition, including cancer (4).

1.1 microRNA biogenesis and mechanism of action

The generation of miRs is a multistage process (4, 5): miRs are transcribed as primary transcripts (pri-miRs) by RNA polymerase II. Each pri-miR contains one or more hairpin structures that are recognized and processed by the microprocessor complex, which consists of the RNase III type endonuclease Drosha and its partner, DGCR8 (Figure 1). The microprocessor complex generates a 70-nucleotide stem loop known as the precursor miR (pre-miR), which is actively exported to the cytoplasm by exportin 5. In the cytoplasm, the pre-miR is recognized by Dicer, another RNase III type endonuclease, and TAR RNA-binding protein (TRBP; also known as TARBP2). Dicer cleaves this precursor, generating a 20-nucleotide mature miR duplex. Generally, only one strand is selected as the biologically active mature miR and the other strand is degraded. The mature miR is loaded into the RNA-induced silencing complex (RISC), which contains Argonaute (Ago) proteins and the single-stranded miR (miRISC). Mature miR allows the RISC to recognize target mRNAs through partial sequence complementarity with its target. In particular, perfect base pairing between the seed sequence of the miR (from the second to the eighth nucleotide) and the seed match sequences in the mRNA 3′ UTR are crucial. The RISC can inhibit the expression of the target

mRNA through two main mechanisms that have several variations: one is the deadenylation, while the other is the translational repression.

Deadenylation of mRNAs is mediated by GW182 proteins which interact with AGOs and act downstream of them.

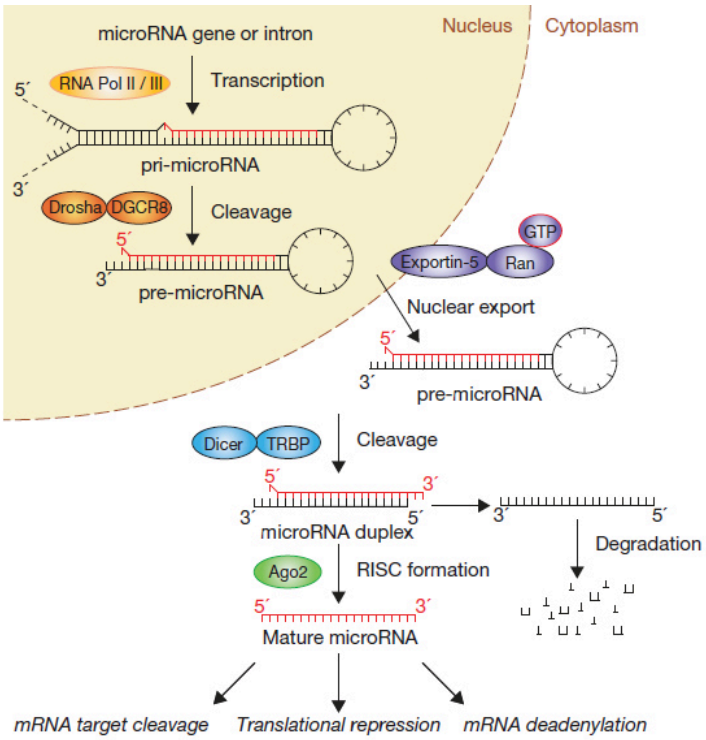

Figure 1 microRNA biogenesis and mechanisms of action

The canonical pathway of microRNA processing (from Winter et al., 2009)

While the amino-terminal part of GW182 interacts with AGO, the carboxy-terminal part of mammalian GW182 proteins interacts with the poly(A) binding protein (PABP) and recruits the deadenylases CCR4 and CAF1 (6). When the miRISC containing AGO2 in mammals encounters mRNAs bearing sites nearly perfectly complementary to miR, these mRNAs are endonucleolytically cleaved and degraded (7).

On the other hand, the translational repression occurs when miRISC and target mRNAs interact with sites of imperfect complementarity. This mechanism affects the cellular translation at the initiation step or at the elongation step. When directed to mRNAs via these

interactions, Ago proteins perform a still incompletely defined activity that results in accelerated turnover and reduced translation of the targeted transcript (7, 8).

1.2 Regulation of microRNAs: expression, stability and intracellular localization

miRs expression can be regulated either through the regulation of miR gene transcription (transcriptional mechanisms) as well as through miR processing (post-transcriptional mechanisms). Transcription of miR genes is regulated in a similar manner to that of protein-coding genes and is a major level of control responsible for tissue-specific or development-specific expression of miRs. The presence of CpG islands, TATA box sequences, initiation elements and certain histone modifications indicates that the promoters of miR genes are controlled by transcription factors (TFs), enhancers, silencing elements and chromatin modifications (6). Many TFs, such as Myc, E2F1 and p53 regulate miR expression positively or negatively in a tissue-specific or developmental-specific manner (9-11). On the other hand, many evidences suggest that the two endoribonucleolytic cleavage steps represent crucial nodes for miR regulation. In the nucleus, Drosha-DGCR8-mediated processing of let-7 pri-miRs can be inhibited by Lin28B (12), whereas the protein hnRNPA1 specifically binds to pri-miR-18a to promote its processing (13). Dicer-mediated processing requires sophisticated regulation and clearly represents another regulatory node (14): Dicer, in association with TRBP and PACT can promote or inhibit the maturation of pre-miRs via 3' end uridylylation (15). Particularly, TRBP binding to Dicer alters dicing kinetics and cleavage site selection, increasing substrate affinity and enzymatic turnover and the generation of miR isoforms (isomiRs) (16, 17). Beyond alteration of the seed sequence, Dicer-mediated tuning of the miR has consequences for guide strand selection (16). Over the last years, increasing attention has been focused on how the regulation of miRs impinges on their stability. The stability of miRs is generally robust and mature miRs persist for hours, or even days, after their production is arrested (18-20). miR recycling can be limited by target regulation, which promotes posttranscriptional modifications to the 3' end of the miR and accelerates the miR's rate of decay (18). Control of steady-state miR concentration directly relates to the control of miR function. Interestingly, although crucial for the regulation of steady-state miR levels, little has been uncovered about the regulation of miR half-life and stability in the cell, following processing. The increased stability of selected miRs is unlikely to be related to a 3' modification of these miRs, as indicated by a recent genome-wide study

that failed to demonstrate an impact of 3' adenylation on miR stability (21). A work by Bail et al. suggests that exosomes can control miR decay in human cells. The exosome 3'-5' exoribonuclease complex was identified as the primary nuclease involved in miR-382 decay with a more modest contribution by the Xrn1 and no detectable contribution by Xrn2 (22).

In addition, argonaute proteins seem to be other key regulators of microRNA stability, increasing microRNA abundance through their stabilization (23). Considerable efforts have been put into establishing whether components of miRISCs are associated with particular cellular structures and whether miR repression can be regulated at this level. P-bodies and stress granules have emerged as being potentially relevant to miR repression, as have multivesicular bodies (MvBs) (6). Blocking MvB formation by depleting endosomal sorting complex required for transport (eSCRT) factors, inhibits miR silencing, whereas blocking MvB turnover by inactivation of the Hermansky–Pudlak syndrome 4 (HSP4) gene stimulates repression by miRs (6). In addition, components of the miRISC loading complex, such as Dicer and AGO2, have been found to be associated with membranous fractions (24, 25). Nucleo-cytoplasm partitioning can also be a determining factor in regulating miRs expression. miR-mediated repression is considered to be a cytoplasmic event, altough substantial amounts of AGO2 and miRs have been found in the nuclei of different mammalian cell lines (26, 27).

1.3 microRNAs in cancer

The first evidence of dysregulation of miR expression in cancer came from a work by Calin et al., in which they discovered that the loss of miR-15a and miR-16-1 was the target of 13q14 deletion that drove chronic lymphocytic leukaemia pathogenesis (28). Following that discovery, expression profiling data of many different types of tumors evidenced that aberrant miR expression is the rule rather than the exception in cancer (29-32). Members of the let-7 family of miRs that map to chromosome regions that are deleted in multiple tumors were found to be lost in multiple different malignancies, including those of lung, breast, urothelial, ovarian and cervical cancers (33).

The miR-17-92 cluster, which maps to a region that is amplified in lymphoma, was found to be overexpressed in many different tumors (32). Interestingly, consistent changes in miR expression were also observed in tumors without evident specific cytogenetic abnormalities, suggesting that pathways commonly dysregulated in human cancer could directly affect and

deregulate miR expression (32). All these evidences contributed to the the discovery that miR-expression profiles can classify human cancers and miR expression fingerprints correlate with clinical and biological characteristics of tumors, including tissue type, differentiation, aggression and response to therapy (30, 34-36).

The general concept is that miRs located in genomic regions that are amplified in cancers function as oncogenes, whereas miRs located in portions of chromosomes deleted in cancers function as tumor suppressors (29, 33). The mechanisms through which miRs expression can be deregulated in cancer are genetic, epigenetic and transcriptional mechanisms (Figure 2). In a fashion similar to protein coding genes, miR genes are also subject to epigenetic changes in cancer mainly related to the methilation status (37-39). Deregulation of miR expression can result from aberrant transcription factor activity in cancer cells (40). To this regard, it has been documented that miR can be suppressed by oncogenic transcription factors as well as by loss of tumor suppressor transcription factors (40).

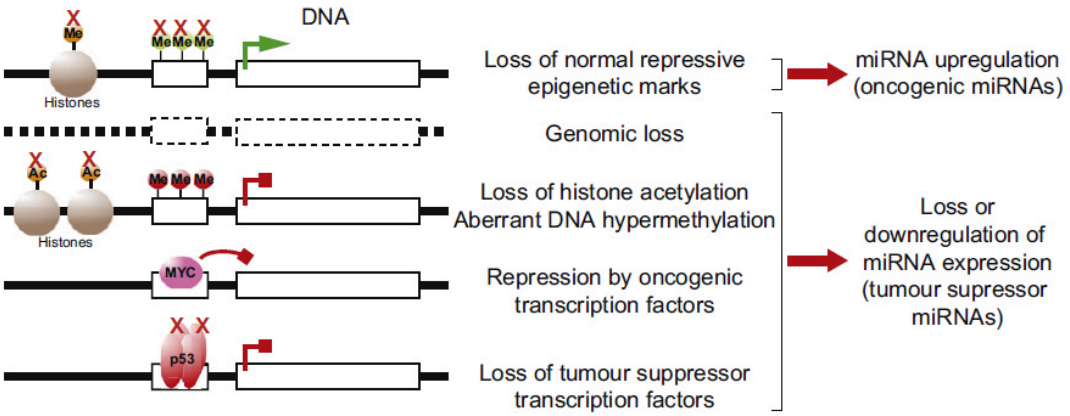

Figure 2 microRNA deregulation in cancer

Deregulation of miR gene transcription in cancer through genetic, epigenetic and transcriptional mechanisms (from Jansson and Lund, 2012)

For example, Myc can down-modulate several microRNAs with documented antiproliferative, pro-apoptotic and tumor suppressor effects, such as let-7, miR-15a/16-1, miR-26a and miR-34 family members (41), while Ras and Zeb1 can modulate miR-143/145 expression and miR-200 respectively (42, 43). On the other hand, transcription of miRs with anti-tumorigenic effects is often activated by transcription factors that are themselves tumor suppressors. One of the best example is represented by p53 that is higly deregulated in cancer

and it can activate the transcription of the miR34 family (44, 45), whose targets include cyclin E2, CDK4 and CDK6, CDC25c, Myc and BCL2 (46).

1.4 microRNAs in cell cycle

Recent evidences suggest that miRs can control the expression of multiple cell cycle regulators and can therefore control cell proliferation (47-49). miRs control cell cycle progression by direct targeting of critical modulators, such as cyclins, CDKs and CDK inhibitors (50-54) (Figure 3).

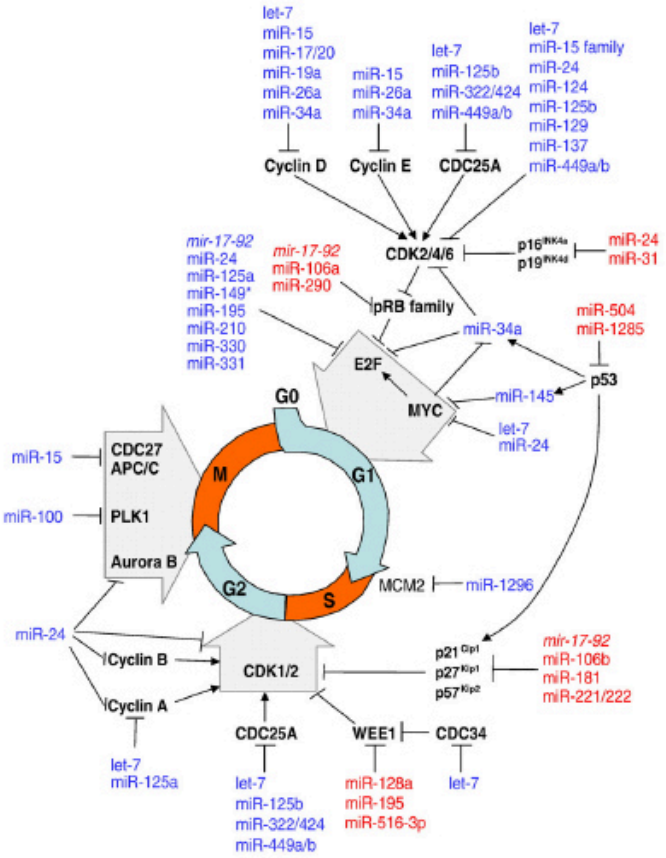

Figure 3 An overview to cell cycle control by microRNAs
(from Bueno and Malumbres, 2011)

Central to cell cycle regulation, the retinoblastoma (pRb) pathway is altered in the vast majority of human cancers (55, 56). Components of the cell cycle machinery such as the

cyclins and cyclin dependent kinases (CDKs) are key targets of growth-suppressing miRs (40, 53). The levels of D-type cyclins are downregulated by let-7, miR-15 family, miR-17, miR-19a, miR-20a, and miR-34 (53). On the other hand, the expression of negative regulators of the cell cycle can be regulated by miRs. To this regard, the role of microRNAs in regulating p27kip1 (hereafter p27) expression is documented in several tumor tissues: the fine tuning of p27 expression during cell cycle entry can be ascribed to miRs 221/222, and the significance of this regulation in cancer progression has been well documented (50, 57). In cells exposed to mitogenic stimuli, when p27 protein expression decreases (58, 59), miR 221/222 expression increases, determining an amplification of pro-mitogenic stimuli that ultimately favors the entrance in S phase (57).

It has been reported that miR-221/222 expression affects the proliferation potential of human prostate carcinoma cell lines by targeting p27 (60). In gastric cancer, miR-196a and miR-148a are upregulated and promotes cell proliferation by downregulating p27 (61, 62). Interestingly, in myeloid cells it was demonstrated that miR-181a regulates cap-dependent translation of p27 (63). Several miRs are known to be induced or repressed by critical transcription factors that control the cell cycle. To this regard, Myc was found to induce the expression of the mir-17-92 cluster (9), while at least four miR clusters (let-7a-d, let-7i, mir-15b-16-2, and mir-106b-25) are direct targets of E2F1 and E2F3 during G1/S and are repressed in E2F1/3 null cells (54). Interestingly, it has been shown that cell cycle progression can affect miR stability (47-49) and transcription (51, 54). Oncogenic miRs, often overexpressed in cancer, can act to facilitate entry and progression through the cell cycle, while tumor suppressor miRs lost in cancers assist in the induction of cell cycle arrest.

1.5 microRNAs in contact inhibition

Widespread gene expression changes occur when cells enter quiescence, including both repression and activation of genes (64-67). Several evidences suggest that the quiescience state (serum deprivation and contact inhibition) relies primarily on the increased expression of the CDK inhibitor p27 (59, 68). Nevertheless, the drivers and mechanisms of the gene expression changes in quiescence are still not known. microRNAs have been implicated in a wide range of biological processes related to quiescence, including cell proliferation control, stem cell renewal, developmental timing, and cancer (69). One of the first evidences about the involvement of microRNAs in the context of cell-cell contact came from the evidence

that the overexpression of one of the component of RISC (SND1) resulted in the irreversible loss of contact inhibition in rat intestinal epithelial cells (70). Recently, it was demonstrated that the quiescent state induced both by serum deprivation and contact inhibition is definitely an active state: microRNAs both increase and decrease in abundance upon entry into quiescence (71). Specifically, the quiescence state is associated with the down-regulation of miR-29 and the consequent release from repression of its targets related to collagen and extracellular matrix proteins (71). On the other hand, the expression of miR-125 and let-7 is induced by quiescence and the overexpression of either one alone resulted in slower cell cycle re-entry from quiescence, while the combination of both together slowed cell cycle re-entry even further (71). Regarding the molecular mechanisms underlying miRs regulation under cell-cell contact, it was found that in diverse animal cell lines, the global efficiency of miR biogenesis is intimately linked to cell density (72). The achievement of high confluence increases both the activity of Drosha and RISC complex, revealing 2 posttranscriptional control points that link miR abundance to cell density (72). Recently, it was demonstrated that a cell cycle regulatory mechanism is involved in the proliferation arrest that follows contact inhibition (73). The final stage of wound closure is preceded in keratinocytes by a strong accumulation of miR-483-3p, which acts as a mandatory signal triggering cell cycle arrest when confluence is reached (73). Similarly, in breast cancer miR-200c downregulates ZEB1 and ZEB2, resulting in an increased formation of stable cell-cell contacts through the modulation of E-cadherin (74).

2 microRNA-223

microRNA-223 (miR-223) was first identified bioinformatically and subsequently characterized in the haematopoietic system, where it is specifically expressed in the myeloid compartment (75, 76).

Few years later, it was demonstrated that miR-223 contains a conserved proximal genomic region that acts as a myeloid-specific promoter that drives miR-223 transcription through the cooperative binding of the transcription factors PU.1 and C/EBP (77).

The role of miR-223 has been described in several papers in hematological malignancies. One of the first evidences, showed that a leukemia fusion protein (Aml1/Eto) could epigenetically silence miR-223 genomic locus driving leukemia pathogenesis (78), and miR-223 down-regulation observed in chronic lymphocytic leukemia was shown as predictive of

treatment-free survival and overall survival (79, 80). Pulikkan et al. described a molecular network in which E2F1 and miR-223 comprise an autoregulatory negative feedback loop in acute myeloid leukemia. In leukemia samples E2F1 is able to physically bind to miR-223 promoter and inhibit its transcription, accounting for miR-223 down-regulation observed in the tumor samples (81). On the other hand, miR-223 over-expression blocks cell cycle progression in leukemia cells by targeting E2F1 (81). Furthermore, miR-223 repression induced by Notch1 expression has been shown to impinge on IGF1R regulation in T-cell acute lymphoblastic leukemia (82).

The use of the knock-out mice for miR-223 strengthened the role of miR-223 in hematopoiesis, revealing that its absence induces neutrophil hyperactivity and the miR-223 mutant mice spontaneously develop inflammatory lung pathology and exhibit exaggerated tissue destruction after endotoxin challenge (83).

Despite its primary role in hematological malignancies, miR-223 has been shown to regulate hepatocellular carcinogenesis as well: a strong down-regulation of miR-223 is observed in hepatocarcinoma samples and its re-expression resulted in a consisted inhibitory effect on cell viability mediated by the repression of stathmin 1 (84). Interestingly, the miR-223 oncosuppressive role has been also observed in esophageal carcinoma where it suppresses a known tumor-metastasis gene (ARTN) eventually decreasing cell migration and invasion (85). Moreover, in osteosarcoma its tumor suppressive function is mediated through the regulation of PI3K/Akt/mTOR pathway (86). Finally, it was demonstrated that miR-223 exerts an oncosuppressive function in glioma as well where miR-223 expression suppresses tumorigenesis in a mechanism mediated by the repression of nuclear factor I-A (NFIA) (87).

In contrast to the well-defined oncosuppressive role of miR-223 in several tissues, some evidences suggest that miR-223 can also act as oncogenic miR, in gastric cancer, where it promotes invasion and metastasis through the targeting of the tumor suppressor EPB41L3 or FBXW7/hCdc4 (88, 89).

Finally, several evidences show that miR-223 can be secreted, has a certain degree of stability and can exert different functions: for instance on one side miR-223 has been recognized as a circulating miR in hepatocellular and in nasopharyngeal carcinoma where it could be used as a biomarker for liver injury and for nasopharyngeal carcinoma detection (90, 91). On the other hand, it can be secreted from macrophages and internalized in breast cancer cells through an exosome-mediated mechanism, eventually promoting invasion of breast tumour cells (92).

3 Cell cycle

The term “cell cycle” defines the process by which a cell correctly divides into two daughter cells, which is central to the understanding of all life (93).

To ensure that DNA faithfully replicates and that the replicated chromosomes correctly segregate into the two newly divided cells, in all eukaryotic cells, cell cycle progression is stringently controlled (94, 95). In particular, several mechanisms ensure that S-phase is completed before mitosis begins and that M phase starts only if the DNA has been faithfully replicated. This is possible since two Gap phases (the G1 separating the M and S-phases, and the G2 between the S and M phases) are present in somatic cells and dictate the timing of cell division during which the control mechanisms principally act. In living organisms the cells are usually in a state of quiescence called G0 and can re-enter into the cell cycle after stimuli derived from the local microenvironment such as growth factors stimulation. The beginning of the G1 phase is the only part of the cell cycle that seems to be dependent on growth factors stimulation. When cells are stimulated by growth factors to enter the cycle from G0, they generally require continuous mitogenic stimulation to be driven to the restriction point, after which mitogens can be withdrawn and cells will enter S-phase and complete the cycle in their absence. At this point, in the G2 phase, before the mitosis (M phase) could start, the cell controls that DNA has been faithful duplicated and checks the internal signalling events necessary for a successful division. Progression of mitosis is controlled by signalling pathways that monitor the integrity of microtubule function, to ensure the fidelity of chromosome segregation. As cells exit mitosis, the cell cycle is reset, allowing the establishment of a new competent replication state in G0 or G1 phase.

3.1 Cyclins and CDKs

Progression through the cell cycle is orderly driven by Cyclin-Dependent Kinases (CDK) activity (Figure 4). CDKs are serine and threonine kinases, and their actions are dependent on associations with their activating subunits, cyclins (96-98). Cyclin abundance is regulated by protein synthesis and degradation and the activity of CDKs is regulated to a large degree by the presence of different cyclins. Cyclin specificity can be achieved in various ways: cyclins are expressed or are present at stable levels at different times; they are differentially sensitive to cell-cycle-regulated inhibitors; they are differentially restricted to specific subcellular locations; or they bind specifically to some phosphorylation targets.

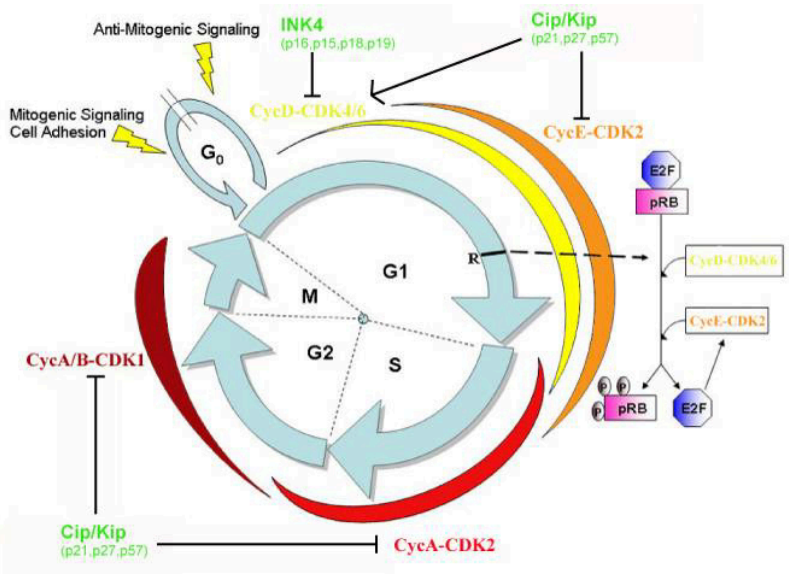

Figure 4. Schematic representation of cell cycle regulation

Mitogenic stimuli promote cell cycle progression from G0 to G1 inducing the expression of D type cyclins and lowering the expression of p27. Sequential activation of cyclin E-CDK2, cyclin A-CDK2, cyclin A-CDK1 and cyclin B-CDK1 allows the cells to pass through the restriction point (R) and to complete the mitotic division. The passage through the R point is due to the inactivation of the pRB protein by CDKs-dependent phosphorylation (from Belletti et al., 2005)

Cyclins are regulated at the level of protein degradation by ubiquitin-mediated proteolysis and this constitutes an important mechanism for cyclin specificity in controlling the cell-cycle machinery.

Restriction point control is mediated by two families of enzymes, the cyclin D- and E-dependent kinases. The D-type cyclins (D1, D2, and D3; 99-100) combinatorially interact with two distinct catalytic partners: CDK4 and CDK6 (101, 102). Whereas CDK4 and CDK6 are relatively long-lived proteins, the D-type cyclins are unstable, and their induction, synthesis, and assembly with their catalytic partners all depend upon persistent mitogenic signalling. The mitogen-dependent accumulation of the cyclin D-dependent kinases triggers the phosphorylation of the Retinoblastoma protein (Rb), thereby helping to cancel its growth-repressive functions (101, 103, 104).

Rb represses the transcription of genes whose products are required for DNA synthesis, such as the E2Fs (105). Rb phosphorylation by the G1 CDKs relieves E2Fs that can act as transcriptional activators. Then, E2Fs can induce cyclin E and A genes. Cyclin E then enters into a complex with its catalytic partner CDK2 (106-109) and collaborates with the cyclin D-dependent kinases to complete Rb phosphorylation (110-112). The activity of the cyclin E-CDK2 complex peaks at the G1-S transition, after which cyclin E is degraded and replaced by cyclin A. Cyclin A is of particular interest among the cyclin family, because it can activate two different CDKs and act in both S and M phases. Finally, the cyclin-CDK complexes are further regulated by the binding to specific CDK inhibitors (113).

3.2 CDK inhibitors

The CDK inhibitors (CKIs) can be divided into 2 families on the basis of their sequence: the INK4 family and the Kip/Cip family (114). The INK4 proteins comprise four members: p15INK4b (115), p16INK4a (116), p18INK4c (117, 118) and p19INK4d (118, 119). The INK4 family inhibits CDK4 and CDK6 by competing for binding with the D-type cyclins (117, 118).

On the other hand, the Kip/Cip family comprises three proteins: p21Cip1/Waf1/Sdi1 (120-122), p27 (68, 123) and p57Kip2 (124, 125). These inhibitors are differently regulated following specific stimuli. p57 is imprinted (125, 126) and has been implicated in cell differentiation (127) and response to stress. p21 transcription is upregulated in response to DNA damage by wild type but not mutant p53, and p27 was initially identified as the factor responsible for inhibiting proliferation in contact-inhibited and TGFβ-treated cells (68, 128). The Kip/Cip family members are 38-44% identical in the first 70 amino acid region of their amino terminus, and this region is sufficient to inhibit cyclin-CDK activity (129-131). The kinase inhibitory domain, in fact, maps to the N-terminus (1-82) and contains the cdk binding site (28-82).

4 Contact inhibition

Contact inhibition is a regulatory mechanism through which cells enter a stage of reversible G1 arrest, that occurs when cells enter in contact with neighbouring cells at high density

(132). While in adult tissues contact inhibition is continuously active and cells arrest in G1 phase, embryonic cells, as well as cells in continuously renewing tissues, are instead less subject to contact inhibition (132, 133). In contrast to most non-transformed adherent cells whose growth usually decreases as cell density increases (133-135), loss of contact inhibition is usually associated with abnormal growth and the appearance of multilayered foci in culture associated with malignant transformation (68, 132, 133). Most human cancer cells are indeed refractory to contact inhibition. As a consequence, they are able to continue proliferation in spite of interactions with neighboring cells and substrata. In more aggressive stages, the dividing cancer cells can invade the surrounding tissue to achieve unlimited growth and can eventually metastasize to secondary sites.

Many established cancer cell lines also exhibit growth in vitro that is impervious to contact inhibition, and often display anchorage-independent growth in soft agar. The loss of contact inhibition and the gain of anchorage-independent growth are hallmarks of cancer cells in vitro (136), suggesting that many oncogenic alterations either uncouple cell proliferation from the mechanism that subjects it to contact inhibition, or alter the contact inhibition mechanism itself.

Contact inhibition is apparently initiated by cell-cell interaction, even if the specific molecular mechanisms are still not well-defined. The characterization of contact-dependent regulation would require the identification of: (***1***) cell surface receptors that are engaged by the physical interaction between cell surfaces; (***2***) growth regulatory signaling pathways that are affected by those receptors in a contact-dependent fashion; and (***3***) molecular mechanisms that functionally and biochemically couple those surface receptors and intracellular signaling pathways together (137). Intercellular adhesion molecules for example, have been shown to be necessary for non-transformed cells growing in a monolayer tissue culture to become quiescent when they reach confluence (138-140).

At this regard, a major role in determining growth arrest at high cell density is played by E-cadherin that is expressed in epithelial tissues where it regulates cell-cell adhesion, cell migration and polarity. Some evidences show that modulation of cadherin-mediated interactions by lowering Ca^{2+} concentration in the culture medium or by inhibitory antibodies, can stimulate cell proliferation (140), whereas overexpression of VE-cadherin, N-cadherin or E-cadherin can inhibit cell growth (141, 142). Furthermore, where cells demonstrated contact inhibition, proliferation was resumed after disrupting E-cadherin function using function-blocking antibodies (143). Studies that first recognized the

phenomenon of contact inhibition also appreciated that, as cultured cells reach confluence, the response to serum growth factors is progressively inhibited despite the continuous replenishment of growth factors in the medium (135). NIH3T3 cells, which are extremely sensitive to contact inhibition (144) exhibit a saturation density that is directly proportional to the serum concentration in which they are grown (145). Studies of EGF-induced and PDGF-induced proliferation in fibroblasts concluded that the ability of cells to respond to individual growth factors decreases with high cell density (146, 147). The EGF receptor (EGFR) was the first member of the receptor tyrosine kinase (RTK) family of growth factor receptors to be identified and was found to localize to lateral cell junctions in confluent cells in a Ca^{2+}-dependent and cadherin-dependent fashion (139). The establishment of contacts between cells elicits a series of signals that are transduced intracellularly and ultimately lead to changes in the expression and/or the activity of genes involved in the regulation of the G1/S transition of the cell cycle. Among the cell cycle regulators, the CDK inhibitor p27 has been implicated in the negative regulation of G1 progression in response to a number of antiproliferative signals, including cell-cell contact (141, 142). Interestingly, contact-induced proliferative arrest mediated by p27 is initiated by the activation of cadherin signalling induced by the establishment of cell-cell contacts (141, 142).

5 p27

p27 plays a crucial role in the G1-S transition by interacting with and inhibiting cyclin E-CDK2 and cyclin A-CDK2 activity, thus blocking cell cycle progression. In early G1, p27 promotes cyclin D-CDK4/6 complex assembly and nuclear import, increasing cyclin D stability, all without inhibiting CDK4 kinase activity. In proliferating cells, p27 is mainly associated with cyclin D-CDK4/6 complexes, but these complexes are catalytically active, whereas in G1 arrested cells p27 preferentially binds and inhibits cyclin E-CDK2. The sequestration of p27 by cyclin D-CDK4/6 complexes effectively releases CDK2 from inhibition, allowing both CDK4/6 and CDK2 to remain active. In this way mitogen induction of cyclin D expression determines cell cycle progression both by activating CDK4 and by sequestering p27 thus favouring cyclin E-CDK2 activation. Once cyclin E-CDK2 is activated, it phosphorylates p27 on Threonine 187, allowing p27 to be recognized by the ubiquitin ligases and targeted for destruction by the 26S proteasomes (148-150). It follows that once cyclin E-CDK2 is activated, p27 is rapidly degraded, contributing to the

irreversibility of passage through the restriction point. If cells are persistently stimulated with mitogens, cyclin D-dependent kinase activity remains high in the subsequent cell cycles, p27 levels stay low, and virtually all of the p27 can be found in complexes with the cyclin D-CDK4/6. However, when mitogens are withdrawn, cyclin D is rapidly degraded, and the pool of previously sequestered Cip/Kip proteins is mobilized to inhibit cyclin E-CDK2, thereby arresting progression generally within a single cycle.

Multiple extracellular stimuli regulate p27 abundance, which functions as a sensor of external signals to cell cycle regulation (Figure 5).

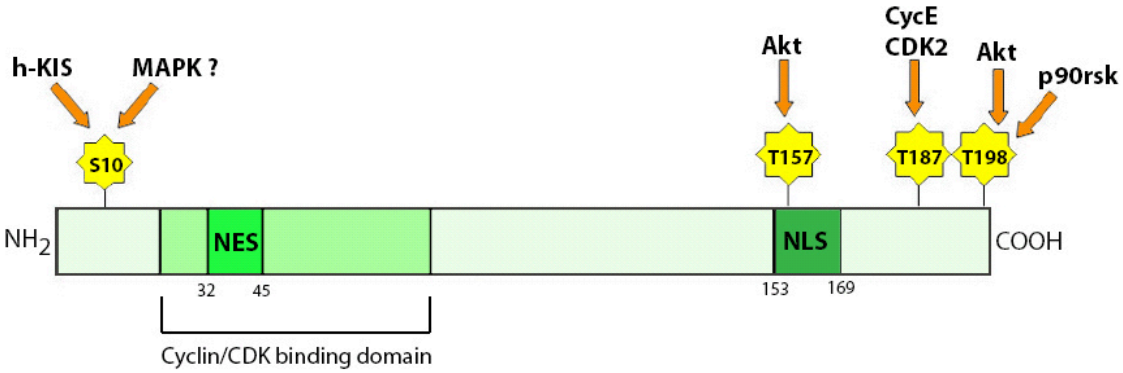

Figure 5 Schematic representation of the principal p27 domains and of its phosphorylation sites (from Belletti et al., 2005)

In normal cells p27 is expressed at high levels in quiescence phase, whereas it decreases rapidly after mitogen triggering and cell cycle re-entry. A number of studies have shown that many anti-mitogenic signals induce the accumulation of p27, including cell-cell contact, growth factor deprivation, loss of adhesion to extracellular matrix, TGF-β, cAMP, rapamycin or lovastatin treatment (151).

5.1 p27 in contact-inhibition

p27 was first identified in cells treated with transforming growth factor TGF-β or in contact inhibited cells where it was found as an inactive form bound to CDK2-cyclin E (68, 128). p27 is an essential component of the pathway that connects mitogenic signals to the cell cycle. Constitutive expression of p27 in cultured cells causes cell cycle arrest in the G1 phase (123). Conversely, its ablation in contact-inhibited cell extracts allows the kinase MO15 to

phosphorylate CDK4 and to activate it, indicating that p27 plays a crucial role in contact inhibition by keeping the Cyclin-D-CDK4 complex inactive (152). Furthermore, the deprivation of serum mitogens in murine BALB/c-3T3 fibroblasts results in p27 accumulation, in the inactivation of G1-cyclin-CDK complexes and cell cycle arrest in G1. Interestingly, the capacity of cells to arrest in response to p27 was found to be governed mainly by cell density (153). Apparently, the proliferation of cells at high density seems to require an event that is inhibited by pocket protein complexes containing Rb and/or p130 (153). Growth of cultures to high density results in G0 arrest, an increase in p27 levels, and a decrease in cyclin/CDK activity. As a consequence, Rb- and p130-containing complexes remain intact, and the expression of gene products required for the proliferation of high-density cells is prevented (153). Another evidence shows that CDK4 and p27 expression are density dependent and contact inhibited cells that achieve the already elevated p27 level are able to maintain a G1 arrest state (154). Interestingly the involvement of p27 in contact inhibition has been observed in several different tissues: in low-grade glioma cells as well as in astrocytes, growth arrest by contact inhibition is accompanied by the induction of p27 expression (155, 156). Human thyroid cancer cell lines are found to be responsive to contact inhibition depending on their ability to upregulate p27 at high cell confluence (143). Strikingly, the antisense inhibition of p27 upregulation at confluence in thyroid cells sensitive to contact inhibition, prevents growth arrest induced by confluence, whereas it has little effect in cells resistant to contact-dependent growth arrest (143). Moreover, the maintenance of a functional E-cadherin/β-catenin complex is necessary for the proper upregulation of p27 and the accomplishment of contact-dependent growth arrest (143). In endothelial cells the induction of the cell-cell contact activated Rac1, up-regulated p27 mRNA and protein, facilitating the cell cycle arrest (157). Interestingly, cell-adhesion-dependent activation of APC/Cdh1 ubiquitin ligase complex, has been found to increase ubiquitination and degradation of Skp2, resulting in a decreased ubiquitination and degradation of p27, and, ultimately, in p27 accumulation, which drives cell-cycle arrest (158).

Aim of the study

Loss of contact inhibition represents a hallmark of cancer. The understanding of the molecular mechanisms that drive the proliferative arrest under high cell-cell contact represents an important issue in the field of cancer biology.

The lack of proliferation arrest when cells are grown at high density is associated with abnormal growth and appearance of multilayered foci in culture. Contact inhibition is characterized by a G1 cell cycle arrest associated with an increase in p27 protein expression. p27 is a cell cycle inhibitor whose main function is to inhibit cell cycle progression at G1/S transition by impairing cyclin E-CDK2 and cyclin A-CDK2 activity. Neverthless, its role and its intracellular partners during contact inhibition have not been clearly elucidated. In the last few years, an increasing number of evidences suggest that the G1 cell cycle arrest is tightly controlled by the expression of several miRs whose interactions with targets can be extremely important for a better understanding of how the complex cell cycle machinery is orchestrated.

In this PhD project we aimed to elucidate the contribution of miRs in the regulation of cell cycle progression, specifically focusing on G1 arrest imposed by contact inhibition and on the role played by p27. We used a microarray approach which revealed that the expression of several microRNAs can be influenced by cell cycle progression.

The data produced during this three years of PhD work describe a novel pathway which couples a key cell cycle regulator, p27, with the regulation of miR expression to control cell cycle exit following contact inhibition.

This new mechanism, which is deranged in human cancer, represents a promising field of future investigation for cancer research and anti-cancer therapeutics, especially in breast cancer.

Results

1 p27 contributes to the regulation of miR-223 expression in G1 arrested cells.

In order to identify miRs potentially regulated by p27 in G1 arrested cells we exploited two strategies. First, using primary mouse embryo fibroblasts (MEF) from WT and p27KO embryos we compared the miR expression profiles in cells collected under exponential growth (EG) *vs* G1 arrested (G1). We identified 59 miRs differentially expressed in WT MEFs between EG *vs* G1 (Figure 6A). Among these, 15 miRs were not in common with the 157 differentially expressed in EG *vs* G1 p27KO MEFs, thus potentially representing the miRs linked to G1 arrest in a p27-dependent manner (Figure 6A). Second, we compared miR profiles from WT MEFs in G1 *vs* S phase (S). 45 miRs were differentially expressed (Figure 6A) and, among them, 8 miRs were in common with the 59 identified in WT MEF, EG *vs* G1 group, reasonably representing miRs specifically modulated by G1 arrest. To select only p27-dependent miRs necessary for the G1 arrest, we compared the group of 15 miRs with the group of 8 miRs (Figure 6A). Three miRs, mmu-miR-223, mmu-miR-712 and mmu-miR-719, were regulated by both G1 arrest and the presence of p27 (Figure 6A). Among them, mmumiR-223 (hereafter miR-223) was the only one with an identified human homolog and was therefore chosen for further analyses. Quantitative RT-PCR (qRT-PCR) analyses on RNA from the same MEF population (Figure 6A, middle graph) and on 4 other independent MEF preparations/genotype (Figure 6B) confirmed the arrays data. G1 arrest, induced either by serum deprivation or by contact inhibition, elicited a marked increase of miR-223 levels in WT MEFs (Figure 6B), although only contact inhibition caused statistically significant differences (Figure 6B). The combined use of serum deprivation and contact inhibition further increased the levels of miR-223 in WT cells (Figure 6B). Transition from G1 to S phase led to progressive decrease of miR-223 levels, similarly to what observed in EG cells (Figure 6B). miR-223 levels paralleled the expression of p27 protein, as demonstrated by immunofluorescence (Figure 6C) or western blot analyses (Figure 6D). When p27KO MEFs were analyzed under the same culture conditions no significant fluctuation in miR-223 levels was observed. Only when contact inhibition and serum deprivation were used together a modest increase in miR-223 expression was appreciated (Figure 6B).

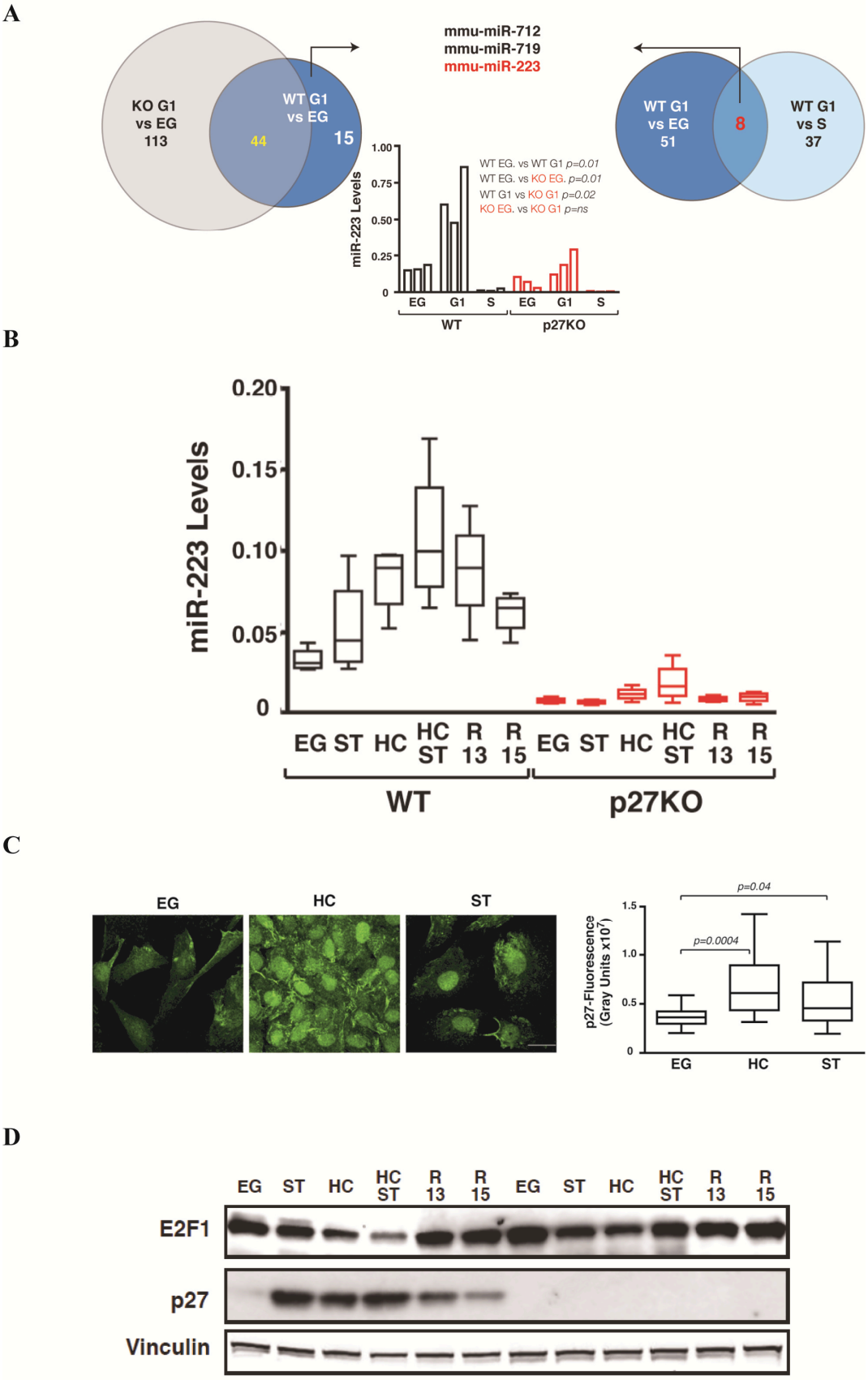
A
KO G1 vs EG 113
WT G1 vs EG
44
15
mmu-miR-712
mmu-miR-719
mmu-miR-223
WT G1 vs EG 51
8
WT G1 vs S 37
miR-223 Levels
1.00
0.75
0.50
0.25
0
WT EG. vs WT G1 p=0.01
WT EG. vs KO EG. p=0.01
WT G1 vs KO G1 p=0.02
KO EG. vs KO G1 p=ns
EG G1 S EG G1 S
WT p27KO
B
miR-223 Levels
0.20
0.15
0.10
0.05
0
EG ST HC HC ST R 13 R 15 EG ST HC HC ST R 13 R 15
WT p27KO
C
EG
HC
ST
p=0.04
p=0.0004
p27-Fluorescence (Gray Units x10^7)
1.5
1.0
0.5
0
EG HC ST
D
EG ST HC HC ST R 13 R 15 EG ST HC HC ST R 13 R 15
E2F1
p27
Vinculin

Figure 6 p27 regulates miR-223 expression following contact inhibition.

A, Schematic representation of miR expression profile analyses. Venn diagram on the left shows numbers of differentially expressed miRs in EG vs G1 WT and p27KO MEF.Venn diagram on the right shows numbers of differentially expressed in EG vs G1and S phase vs G1 WT MEF. In the graph, qRT-PCR validation of miR-223 expression in the same MEF population used for the array is reported. Data represent the $2^{-\Delta CT}$ values obtained by normalizing miR-223 with snoRNA234 expression. **B**, miR-223 expression in 4 independent MEF preparations/genotype, cultured as indicated. Data represent the $2^{-\Delta CT}$ values obtained by normalizing miR-223 with U6 expression. **C**, Immunofluorescence analyses of p27 expression and localization (green) in primary MEFs fixed in exponential growth (EG), high confluence (HC) or serum starved (ST) conditions. On the right, box plot quantification of p27 fluorescence, calculated using the Volocity program (Perkin Elmer) in at least 50 independent cells/condition, expressed as fluorescence gray units. Significance was calculated using the Mann-Whitney unpaired t-test. **D**, Western blot analyses of E2F1 and p27 expression in WT and p27KO MEFs harvested in the indicated culture conditions. EG = Exponentially growing cells; ST= Serum Starved; HC= High Confluence; HC ST, starved and grown at high confluence; R13/R15= Cells blocked in G1 by serum starvation and high confluence and then released in complete medium for 13 or 15 hours. Vinculin was used as loading control. In the lower graph, levels of miR-223 in the same conditions are reported. Abbreviations in this figure are: G1= cells arrested in G1 phase of the cell cycle by contact inhibition and serum deprivation for 24 hours; EG = Exponentially growing cells; S= S phase cells collected 10 hours after release from a double thymidine block. ST= Serum Starved; HC= High Confluence; HC ST, grown at high confluence and serum starved; R13/R15= Cells blocked in G1 by serum starvation and high confluence and then released in complete medium for 13 or 15 hours.

2 p27 is a critical mediator of miR-223 expression after contact inhibition.

Next, we investigated in more detail the regulation of miR-223 by p27 in G1 arrested cells following contact inhibition. By exposing WT MEFs for 24 hours to conditioned medium harvested from WT MEFs under EG or highly confluent (HC) conditions, we excluded that secreted/diffusible factors produced in HC could induce miR-223 expression (Figure 7A). Conversely, by splitting cells from HC culture into low or high confluence conditions (Figure 7B) or by treating HC cells with EGTA to disrupt the cell-cell contacts (Figure 7C), we observed that cell-cell contact was necessary in WT but not in p27KO MEFs to sustain the expression of miR-223.

3 miR-223 stability is affected by transcriptional and post-transcriptional mechanisms.

To dissect the mechanism whereby p27 regulated miR-223 expression following contact inhibition we blocked RNA transcription with Actinomycin D (Act-D) and measured the levels of miR-223. In HC WT MEFs miR-223 remained stable over time even in the presence of Act-D, while its levels significantly decreased in p27KO cells (Figure 8A). The use of α-amanitin, a specific inhibitor of RNA Polymerase II, which is responsible of miRs transcription (159), confirmed these data. Both in WT and p27KO MEFs α-amanitin completely blocked pri-miR-223 expression (Figure 8B), but only in p27KO MEFs mature miR-223 levels dropped after treatment (Figure 8C), suggesting that the expression of p27 was necessary for the stability of mature miR-223. Accordingly, when pre-miR-223 was ectopically expressed under the control of an exogenous CMV promoter and cell-cell contacts were disrupted by EGTA treatment, levels of miR-223 remained stable in WT while they dropped in p27KO MEFs (Figure 8D).

4 A miR-223/E2F1 regulation loop controls cell cycle exit after contact inhibition.

The above data suggested that cell-cell contact triggered miR-223 transcription, which was eventually stabilized by p27 expression. To validate this hypothesis we measured the levels of endogenous pri-miR-223 demonstrating that pri-miR-223 levels increased in HC conditions in both WT and p27KO cells (Figure 9A). These data implied that in primary MEFs contact inhibition directly signaled on the miR-223 promoter, in a manner at least partially independent from p27 expression.

A

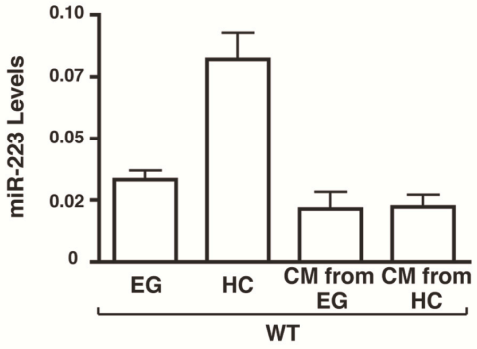
miR-223 Levels
0.10
0.07
0.05
0.02
0
EG
HC
CM from EG
CM from HC
WT

B

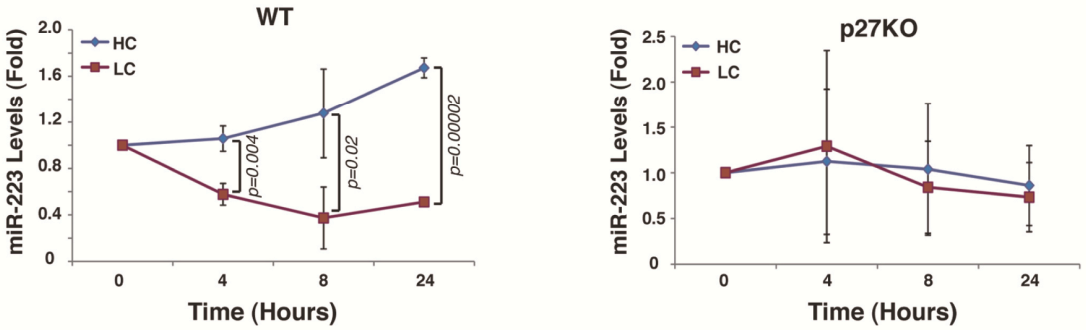
WT
HC
LC
miR-223 Levels (Fold)
2.0
1.6
1.2
0.8
0.4
0
p=0.004
p=0.02
p=0.00002
0
4
8
24
Time (Hours)
p27KO
HC
LC
miR-223 Levels (Fold)
2.5
2.0
1.5
1.0
0.5
0
0
4
8
24
Time (Hours)

C

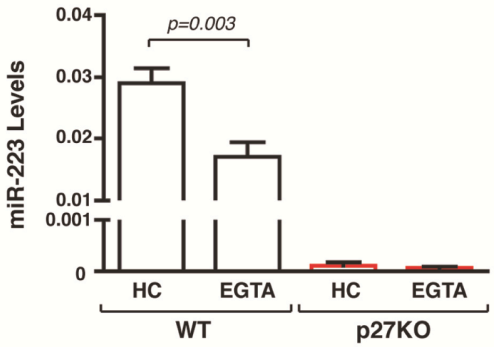
p=0.003
miR-223 Levels
0.04
0.03
0.02
0.01
0.001
0
HC
EGTA
HC
EGTA
WT
p27KO

Figure 7 p27kip1 is a critical mediator of miR-223 expression after contact inhibition.
A, miR-223 expression in 3 independent MEF preparations cultured in EG or HC condition or in EG condition in the presence of conditioned medium (CM) from EG or HC cells as indicated. Data represent the $2^{-\Delta CT}$ values obtained by normalizing miR-223 with U6 expression. **B,** miR-223 expression in 3 independent WT (left graph) or p27KO (right graph) MEF preparations cultured in HC, then split and replated at high (HC) or low (LC) confluence for up to 24 hours. Data are expressed as fold increase of miR-223 respect to the T0 (HC harvested cells). p values were obtained by unpaired student t-test, using either Excel or Prism softwares. **C**, miR-223 expression in 3 independent WT or p27KO MEF preparations cultured in HC condition and then treated with EGTA for 1 hour. Data represent the $2^{-\Delta CT}$ values obtained by normalizing miR-223 with U6 expression.

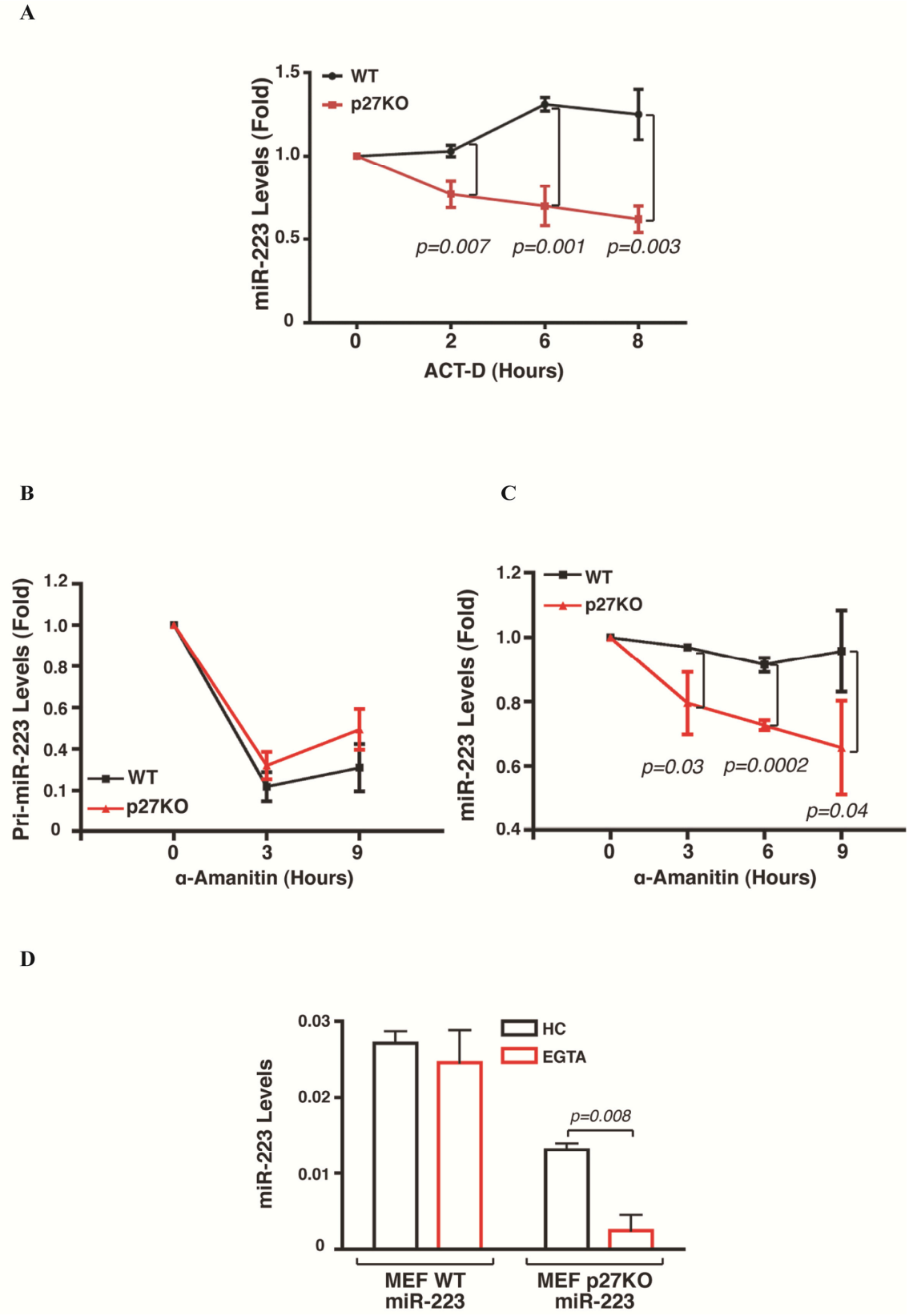
A
WT
p27KO
miR-223 Levels (Fold)
1.5
1.0
0.5
0
p=0.007
p=0.001
p=0.003
0
2
6
8
ACT-D (Hours)
B
Pri-miR-223 Levels (Fold)
1.2
1.0
0.8
0.6
0.4
0.1
0
WT
p27KO
0
3
9
α-Amanitin (Hours)
C
WT
p27KO
miR-223 Levels (Fold)
1.2
1.0
0.8
0.6
0.4
p=0.03
p=0.0002
p=0.04
0
3
6
9
α-Amanitin (Hours)
D
miR-223 Levels
0.03
0.02
0.01
0
HC
EGTA
p=0.008
MEF WT
miR-223
MEF p27KO
miR-223

Figure 8 miR-223 stability is affected by transcriptional and post-transcriptional mechanisms.

A, miR-223 expression in 3 independent WT or p27KO MEFs preparations cultured in HC condition in the presence or not of actinomycin-D (ACT-D) for up to 8 hours. Data are expressed as fold increase of miR-223 levels respect to the T0 (HC harvested cells). **B**, and **C**, pri-miR-223 (B) or miR-223 (C) expression in 3 independent WT or p27KO MEF preparations cultured in HC in presence or not of α-amanitin, for up to 9 hours. Data are expressed as fold increase of pri-miR-223/miR-223 levels respect to the T0 (HC harvested cells). **D**, miR-223 expression in WT and p27KO MEFs transduced with lentiviruses encoding for pre-miR-223 under the control of a CMV promoter, cultured in HC condition and then treated with EGTA for 1 hour. Data represent the $2^{-\Delta CT}$ values obtained by normalizing miR-223 with U6 expression.

A

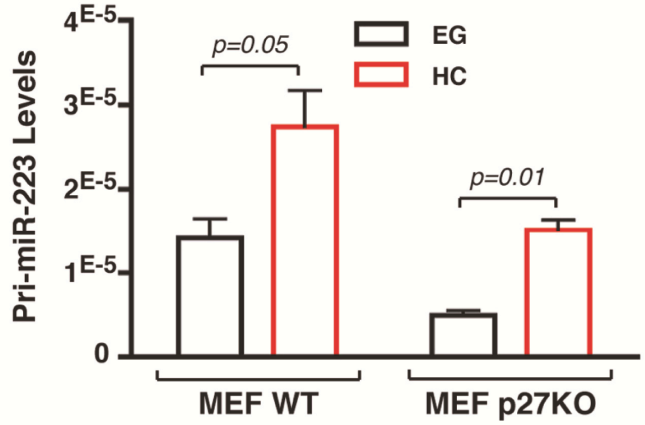
Pri-miR-223 Levels
4E-5
3E-5
2E-5
1E-5
0
p=0.05
p=0.01
EG
HC
MEF WT
MEF p27KO

B

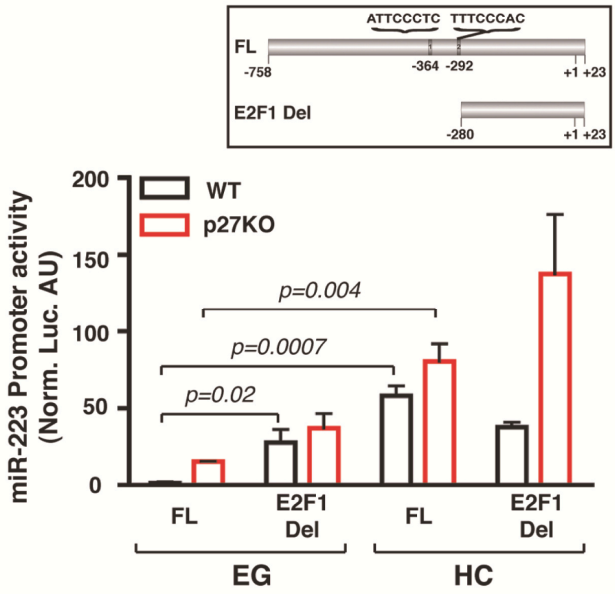
ATTCCCTC
TTTCCCAC
FL
-758
-364
-292
+1
+23
E2F1 Del
-280
+1
+23
miR-223 Promoter activity
(Norm. Luc. AU)
200
150
100
50
0
WT
p27KO
p=0.004
p=0.0007
p=0.02
FL
E2F1 Del
FL
E2F1 Del
EG
HC

C

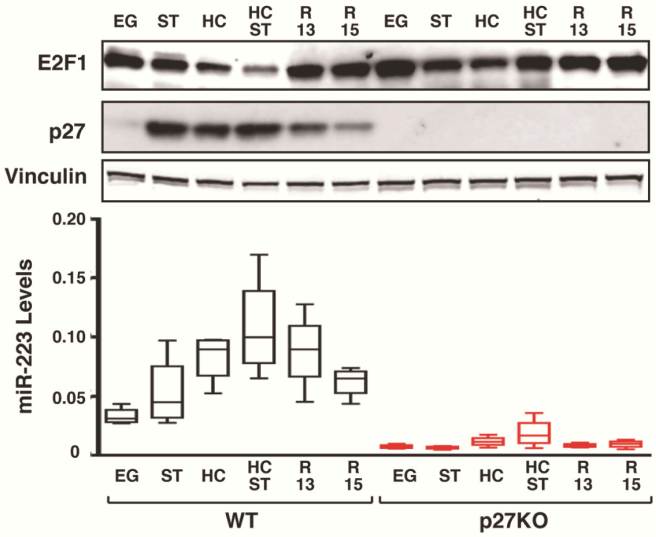
EG
ST
HC
HC ST
R 13
R 15
E2F1
p27
Vinculin
miR-223 Levels
0.20
0.15
0.10
0.05
0
WT
p27KO

Figure 9 Contact inhibition regulates miR-223 transcription.

A, Pri-miR-223 normalized expression in 3 independent WT or p27KO MEF preparations, cultured in Exponential Growth (EG) or High Confluence (HC). **B**, miR-223 promoter activity in WT and p27KO cells grown in EG or HC conditions. In the inset, miR-223 promoter constructs used are depicted. FL= full length; E2F1 Del= deleted of the 2 putative E2F1 binding sites. **C**, Western blot analysis of E2F1 and p27 expression in WT and p27KO MEFs harvested at the indicated culture conditions. Vinculin was used as loading control. In the lower graph, miR-223 expression levels in the same culture conditions are reported. EG = Exponentially growing cells; ST= Serum Starved; HC=High Confluence; HC ST, starved and grown at high confluence; R13/R15= Cells blocked in G1 by serum starvation and high confluence and then released in complete medium for 13 or 15 hours.

Indeed, achievement of cell confluence increased mouse miR-223 promoter activity in both WT and p27KO cells, as judged by luciferase reporter assay (Figure 9B). It has been proved that the transcription factor E2F1 binds and represses miR-223 promoter in human acute myeloid leukemia (AML) (81) and that miR-223 promoter regulation is conserved among human and mouse (77, 78). Given the established role of E2F1 in cell cycle progression (160), we tested whether cell-cell contact regulated miR-223 promoter activity via E2F1. This hypothesis was confirmed by several observations. In WT cells E2F1 was regulated by cell-cell contact and its expression levels inversely correlated with those of miR-223 (Figure 9C). The deletion of two putative E2F1 binding sites in the miR-223 promoter (E2F1Del in Figure 9B) significantly increased its activity in WT cells, only when cultured in EG condition. This effect was specifically due to the two predicted-E2F1 binding sites since similar results were obtained when these two E2F1 binding sites were point mutated (Figure 10A). In contrast, deletion of E2F1 sites increased miR-223 promoter activity in p27KO cells both in EG and HC, although differences did not reach statistical significance (Figure 9B). The latter observation was in accord with endogenous protein levels, demonstrating that in HC p27KO cells E2F1 expression was not completely downmodulated (Figure 9C). Bioinformatic analyses highlighted the presence of a conserved site for miR-223 binding in the mouse E2F1 3'UTR (not shown), as previously demonstrated in human AML (78), supporting the possibility that also in mice a feedback regulation loop exists. Western blot and qRT-PCR analyses proved that in HC WT MEFs miR-223 knock-down resulted in the upregulation of E2F1 (2.9 folds) (Figure 10B). Conversely, in S phase WT MEFs, when miR-223 levels dropped and E2F1 expression raised (Figure 9C), miR-223 overexpression resulted in a significant downregulation of E2F1 protein (Figure 10B, right panels). Importantly, this feedback regulation loop played critical a role in the regulation of cell cycle entry and exit. Indeed, in WT cells miR-223 knock-down partially rescued the G1 arrest imposed by contact inhibition (Figure 11A) and miR-223 overexpression delayed of about 3 hours the S phase entrance of serum starved MEF following serum stimulation, as demonstrated by BrdU assay and FACS analyses of cell cycle distribution (Figure 11B and C). Our and literature data demonstrated that WT and p27KO MEFs equally arrested following contact inhibition (161 and data not shown), although p27KO cells showed a faster entrance into the cell cycle following serum stimulation (162 and Figure 11D).

A

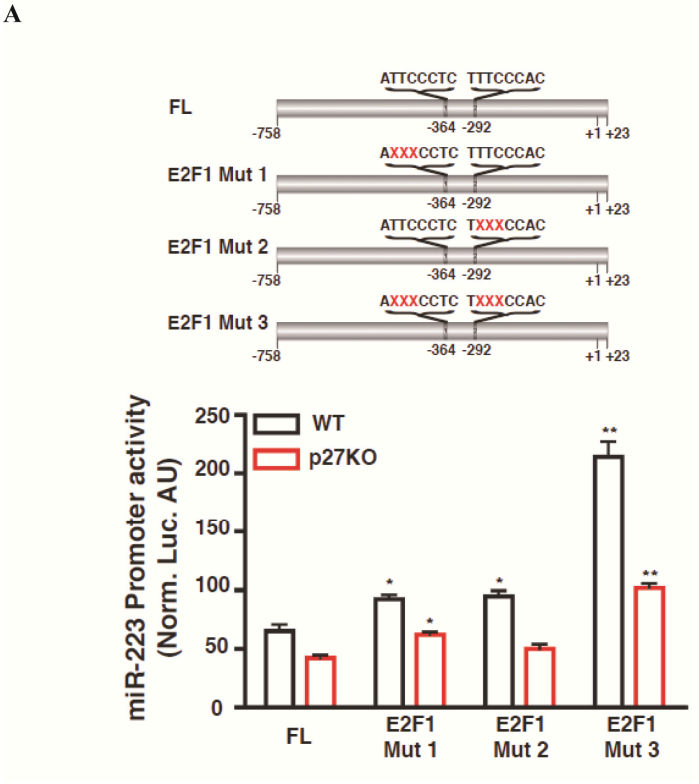
ATTCCCTC TTTCCCAC
FL
-758
-364 -292
+1 +23
AXXXCCTC TTTCCCAC
E2F1 Mut 1
ATTCCCTC TXXXCCAC
E2F1 Mut 2
AXXXCCTC TXXXCCAC
E2F1 Mut 3
miR-223 Promoter activity (Norm. Luc. AU)
250
200
150
100
50
0
WT
p27KO
E2F1 Mut 1
E2F1 Mut 2
E2F1 Mut 3

B

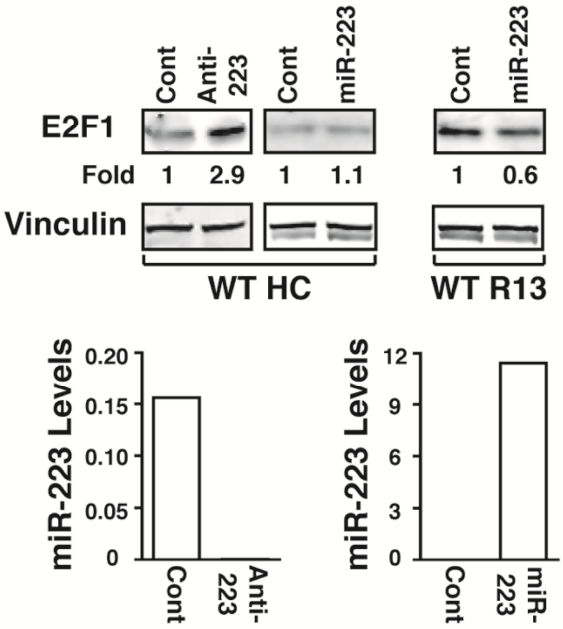
Cont
Anti-223
miR-223
E2F1
Fold 1 2.9 1 1.1 1 0.6
Vinculin
WT HC
WT R13
miR-223 Levels
0.20
0.15
0.10
0.05
0
12
9
6
3
Cont
Anti-223
miR-223

Figure 10 A miR-223/E2F1 regulation loop controls cell cycle exit after contact inhibition.

A, miR -223 promoter activity in WT and p27KO cells. On the top, the miR-223 promoter constructs used are depicted. FL= full length; E2F1 Mut 1= mutation of the first E2F1 binding site; E2F1 Mut 2= mutation of the second E2F1 binding site; E2F1 Mut 3= mutation of both E2F1 binding sites. **B**, Western blot analyses of E2F1 expression in WT HC and WT R13 cells transfected with anti-miR or miR mimics, as indicated. In the lower graph, levels of miR-223 in control and transfected cells are reported. Data represent the $2^{-\Delta CT}$ values obtained by normalizing miR-223 with U6 expression.

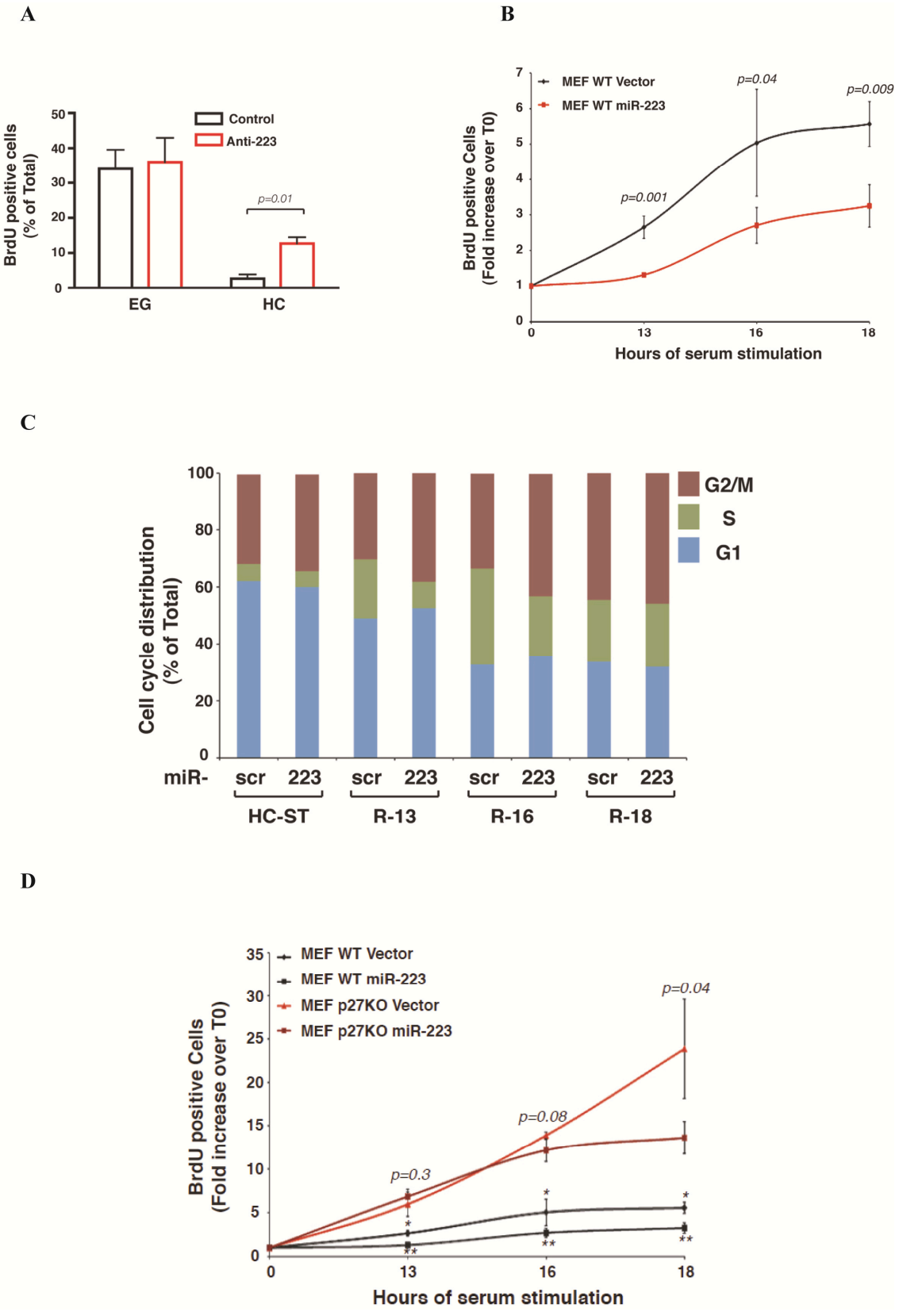
A
BrdU positive cells (% of Total)
Control
Anti-223
p=0.01
EG
HC
B
BrdU positive Cells (Fold increase over T0)
MEF WT Vector
MEF WT miR-223
p=0.001
p=0.04
p=0.009
Hours of serum stimulation
C
Cell cycle distribution (% of Total)
G2/M
S
G1
miR-
scr
223
HC-ST
R-13
R-16
R-18
D
BrdU positive Cells (Fold increase over T0)
MEF WT Vector
MEF WT miR-223
MEF p27KO Vector
MEF p27KO miR-223
p=0.3
p=0.08
p=0.04
Hours of serum stimulation

Figure 11 miR-223 controls cell cycle exit in WT MEFs.

A, BrdU incorporation assay of WT MEFs transfected with anti-miR-223 (Anti-223) or control oligo (Control), grown at EG or HC. Percentage of BrdU positive cells in each condition from two different MEF preparations is reported. **B**, BrdU incorporation assay of WT MEF overexpressing or not miR-223, grown at high confluence, serum starved (HC-ST) and released in complete medium for 13, 16, 18 hours. Data are expressed as fold induction respect to T0 (HC-ST) and represent the mean (±SD) values obtained from three different MEFs preparation. **C**, Cell cycle distribution of WT MEF overexpressing or not miR-223, grown at high confluence and serum starved (HC-ST) and released in complete medium for 13, 16, 18 hours (R-13, R-16, R-18), measured by FACS analysis. Data represent the mean values obtained from two different MEFs preparation/treatment.

D, BrdU incorporation assay of WT and p27KO MEF overexpressing or not miR-223, grown at high confluence and serum starved (HC-ST) and released in complete medium for 13, 16, 18 hours (R-13, R-16, R-18). Data represent the mean of two different MEFs preparation/treatment.

However, overexpression of miR-223 had only a partial effect on p27KO MEFs cell cycle entry (Figure 11D), suggesting that other mechanisms were also implicated or that compensatory mechanisms existed in p27 null cells.

5 p27 is a RNA binding protein and directly stabilizes miR-223.

Data collected so far did not account for the differences observed in the stability of the mature miR-223 between WT and p27KO cells. To get more insights in the regulation of miR-223 stability by p27, we overexpressed p27 wild type (p27WT) or p27CK- and p27KR mutants in p27KO 3T3 fibroblasts (Figure 12A and B). p27CK- is unable to bind the Cyclin/CDK complexes, thus it does not block the phosphorylation of Retinoblastoma proteins (163). p27KR carries two point mutations (K165A and R166A) in the nuclear localization signal and therefore preferentially locates into the cytoplasm (164). All exogenously expressed p27 proteins were able to significantly increase the levels of endogenous miR-223 in p27KO cells (Figure 12C), demonstrating that the extent of miR-223 increase was not influenced by the loss of nuclear localization or by the loss of cyclin/CDK binding ability and suggesting that p27 stabilized miR-223 expression via a cytoplasmic and CDK-independent activity. These data prompted us to use an *in vitro* degradation assay in which cell lysates from p27 null cells were used to test the half-life of a synthetic miR-223 oligo, in the presence or not of recombinant p27. This assay demonstrated that *in vitro*, the recombinant p27 protein was able to significantly lengthen the half-life of miR-223 but not of control-miR or of the un-related miR-1 (Fig 13A and B), suggesting the hypothesis that p27 directly bound and protected from degradation miR-223. This possibility was supported by the *in silico* analyses (BindN prediction program) showing that both human and mouse p27 proteins contains several putative RNA binding domains (Figure 13C). Using RNA immunoprecipitation (RIP) assay, we then assessed that human p27 was able to bind miR-223 in a cytoplasmic and CDK- independent manner, by a region comprised between aminoacids (aa) 86 and 154 (Figure 14 A-C). Two putative RNA-binding sites are present in this region and one of them is highly conserved among mammals (Figure 15A). The most conserved RNA binding site was the region comprised between aa 86 and 154 (Figure 14A-C and 15A). *In silico* analyses demonstrated that three point mutations in R93, P95 and K96 would be sufficient to completely disrupt this binding site (Figure 15B). We thus generated this mutant (hereafter called p27MUT1) and demonstrated that it barely binds miR-223,

with an affinity below the threshold we set as significant when the fold enrichment was calculated (Figure 15C). Next, we tested the possibility that also the region between aa 134 and 142 could bind miR-223. In doing so, we took advantage of the notion that in human breast cancer it has been recently isolated a mutant form of p27 carrying one base deletion at codon 134, resulting in the frameshift of p27 open reading frame and in a truncated protein. We generated this mutant, named p27K134fs and our RIP assay demonstrated that it is still able to bind miR-223, although with very low affinity (Figure 15C). When the two RNA binding site where concomitantly destroyed (p27dMUT mutant) (Figure 15A and C) we observed no binding between p27 and miR-223. These data suggested that miR-223 could bind primarily the region between aa 86 and 154 that it is highly conserved among species, and that the region between aa 134 and 142 could participate in the binding (Figure 15A). Accordingly, RIP performed on endogenous p27 immunoprecipitated from HC or EG WT and p27KO MEFs confirmed that miR-223 was readily recovered only in WT HC cells (Figure 15D).

6 Regulation of miR-223 by p27 in breast cancer.

Loss of contact inhibition is a hallmark of cancer and the role of p27 is of particular importance during breast cancer progression. The CDKN1B gene, encoding for p27, has been found mutated in some histotypes and deregulated in others (reviewed in 114, 165). Moreover, p27 deregulated expression is often considered a negative and independent prognostic factor in cancer. We thus evaluated the expression of p27 and miR-223 in a panel of breast cancer derived cell lines, grown in EG or HC. p27 was considerably upregulated by contact inhibition only in fibroadenoma-derived MCF10A cells (a model of semi-normal mammary gland epithelial cells) (Figure 16A) and this was paralleled by upregulation of miR-223. In contrast, in tumor-derived cells miR-223 expression was not modified by contact inhibition (Figure 16B), suggesting that p27 could affect miR-223 regulation in mammary epithelial cells and that it could contribute to loss of miR-223 in breast cancer. To test this hypothesis, we interrogated The Cancer Genome Atlas (TCGA) data set, containing miR expression in 83 normal breast tissues and 697 breast cancers (166). miR-223 levels were generally reduced in the different types of breast cancers, with the exception of Triple Negative Breast Cancer (TNBC) (Figure 16C).

A

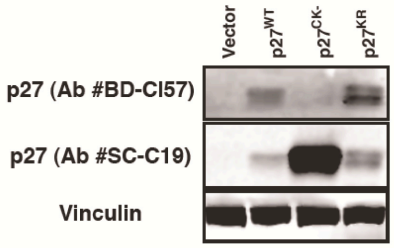
Vector
p27WT
p27CK-
p27KR
p27 (Ab #BD-Cl57)
p27 (Ab #SC-C19)
Vinculin

B

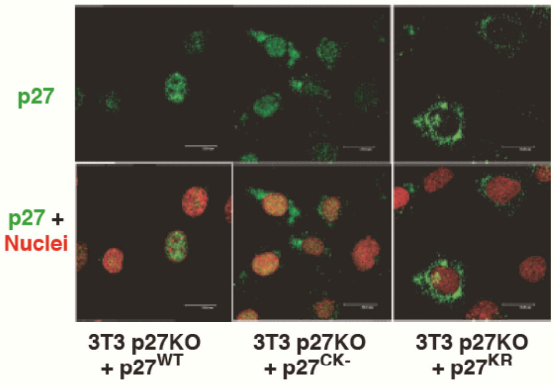
p27
p27 +
Nuclei
3T3 p27KO
+ p27WT
3T3 p27KO
+ p27CK-
3T3 p27KO
+ p27KR

C

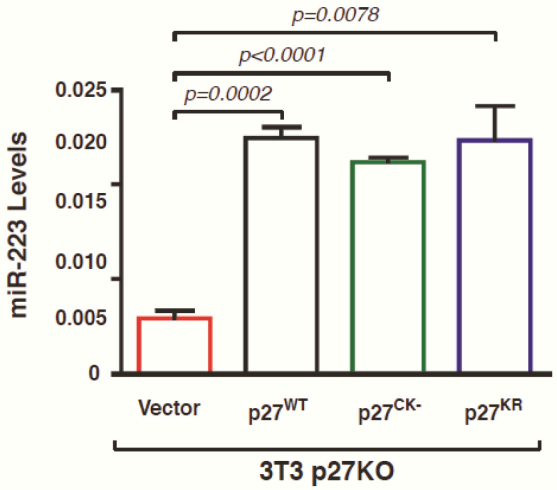
p=0.0078
p<0.0001
p=0.0002
miR-223 Levels
0.025
0.020
0.015
0.010
0.005
0
Vector
p27WT
p27CK-
p27KR
3T3 p27KO

Figure 12 p27kip1 stabilizes miR-223 expression via a cytoplasmic and CDK-independent activity.

A, Western blot analyses of p27 expression in 3T3 p27KO fibroblasts transfected with the indicated p27 mutants. Two different anti-p27 antibodies were used to recognize mutants: Ab#BD-Cl57, raised against the CDK binding domain of p27, does not recognize the CK- mutant. Ab#SC-C19, raised against the C-terminus of p27, recognizes the CK- mutant. **B**, Immunofluorescence analyses of p27 expression and localization (green) in 3T3 p27KO, transfected as indicated. The propidium iodide staining of the nuclei is shown in red. **C**, miR-223 expression in p27KO 3T3 fibroblasts transduced with retroviruses encoding for p27WT, p27CK- and p27KR, as indicated. Data represent the $2^{-\Delta CT}$ values obtained by normalizing miR-223 with U6 expression. p values were obtained by unpaired student t-test, using either Excel or Prism softwares.

A

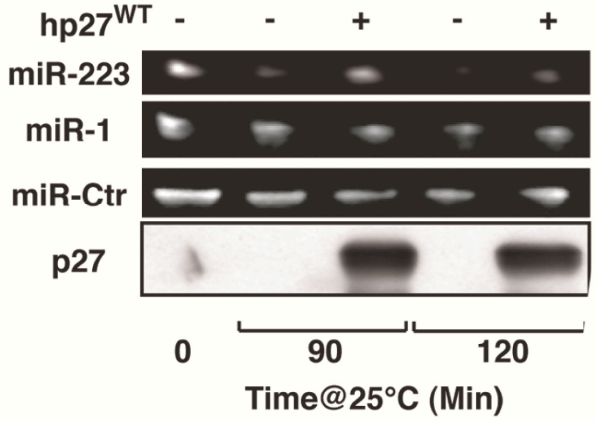
hp27WT - - + - +
miR-223
miR-1
miR-Ctr
p27
0
90
120
Time@25°C (Min)

B

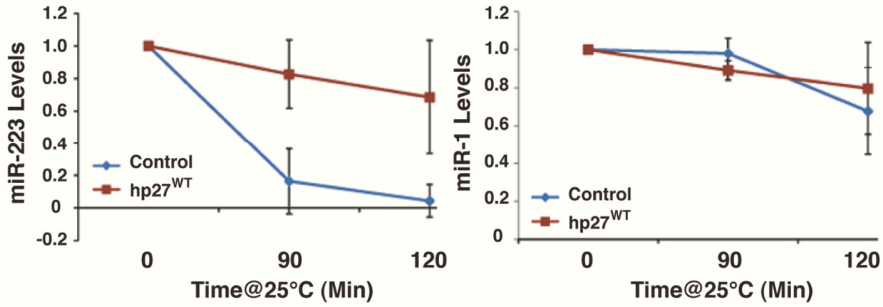
miR-223 Levels
1.2
1.0
0.8
0.6
0.4
0.2
0
-0.2
Control
hp27WT
0
90
120
Time@25°C (Min)
miR-1 Levels
1.2
1.0
0.8
0.6
0.4
0.2
0
Control
hp27WT
0
90
120
Time@25°C (Min)

C

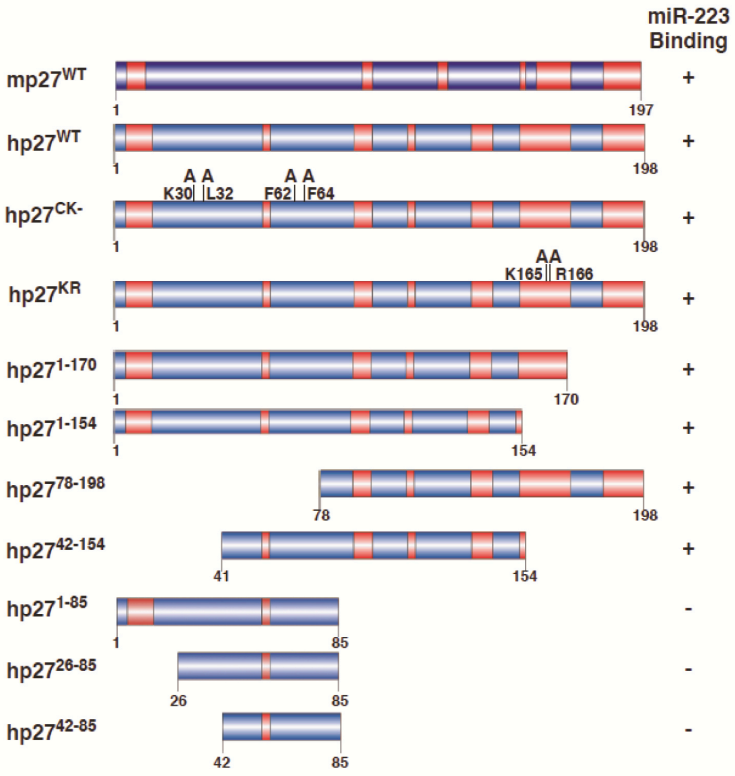
miR-223 Binding
mp27WT
1
197
+
hp27WT
1
198
+
A A
K30 L32
A A
F62 F64
hp27CK-
1
198
+
AA
K165 R166
hp27KR
1
198
+
hp27 1-170
1
170
+
hp27 1-154
1
154
+
hp27 78-198
78
198
+
hp27 42-154
41
154
+
hp27 1-85
1
85
-
hp27 26-85
26
85
-
hp27 42-85
42
85
-

Figure 13 p27kip1 stabilizes mature miR-223 by preventing its degradation.

A, *In vitro* miR degradation assay. Expression of miR-223, miR-1, control miR and p27 protein after 0, 90 and 120 minutes of incubation with lysate from p27KO cells is reported. Human recombinant p27 protein was added where indicated. **B**, Quantification of miR-223 (left graph) and miR-1 (right graph) levels from the in vitro miR degradation assay described in (A). Data represent the mean of three experiments performed in duplicate and are expressed as fold of miR levels respect to T0. **C**, Schematic representation of EGFP-fusion proteins used in RIP assays, based on *in silico* prediction results from BindN software.

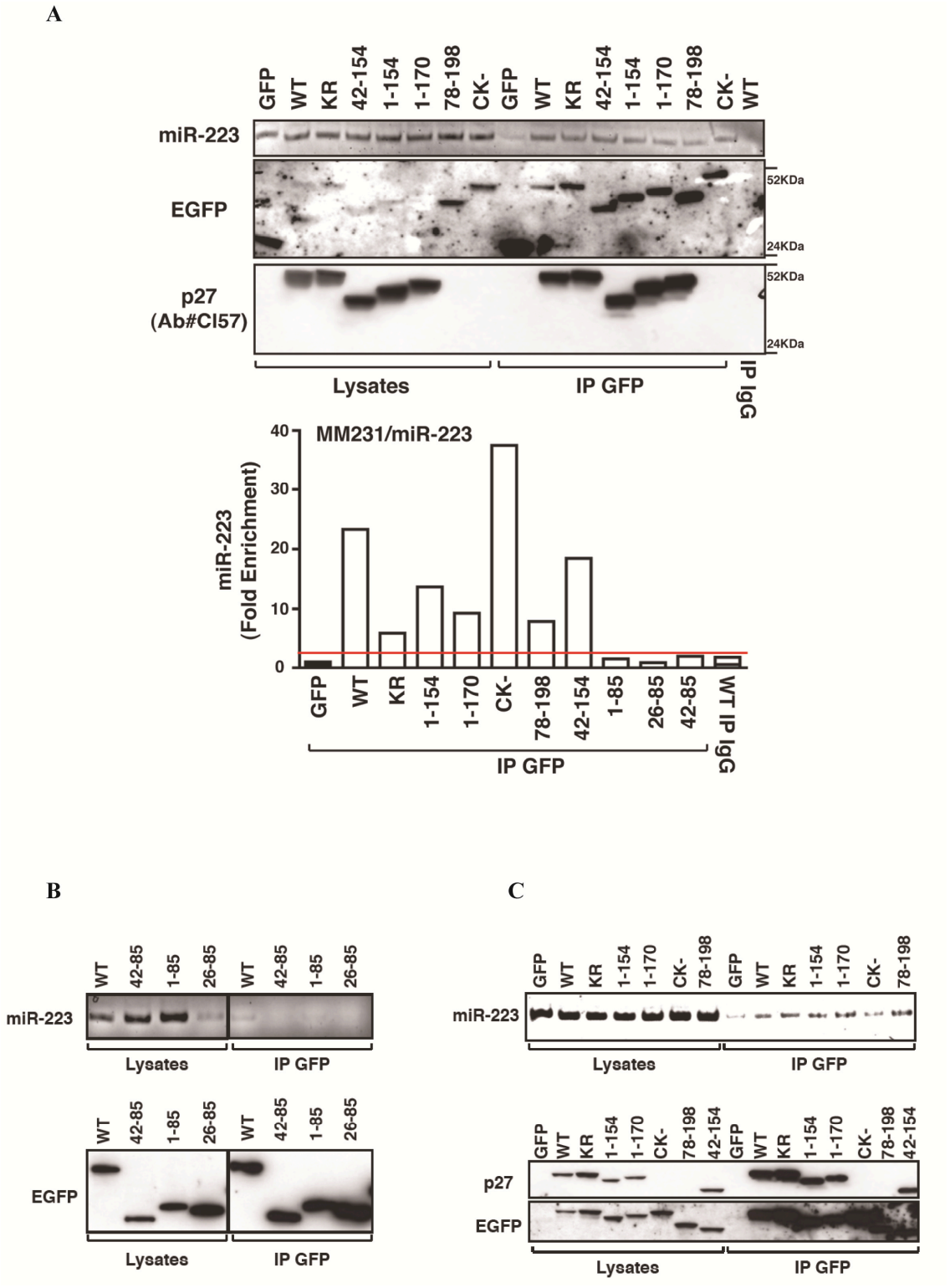
A
GFP
WT
KR
42-154
1-154
1-170
78-198
CK-
GFP
WT
KR
42-154
1-154
1-170
78-198
CK-
WT
miR-223
EGFP
52KDa
24KDa
p27
(Ab#Cl57)
52KDa
24KDa
Lysates
IP GFP
IP IgG
MM231/miR-223
miR-223
(Fold Enrichment)
40
30
20
10
0
GFP
WT
KR
1-154
1-170
CK-
78-198
42-154
1-85
26-85
42-85
WT IP IgG
IP GFP
B
WT
42-85
1-85
26-85
WT
42-85
1-85
26-85
miR-223
Lysates
IP GFP
WT
42-85
1-85
26-85
WT
42-85
1-85
26-85
EGFP
Lysates
IP GFP
C
GFP
WT
KR
1-154
1-170
CK-
78-198
GFP
WT
KR
1-154
1-170
CK-
78-198
miR-223
Lysates
IP GFP
GFP
WT
KR
1-154
1-170
CK-
78-198
42-154
GFP
WT
KR
1-154
1-170
CK-
78-198
42-154
p27
EGFP
Lysates
IP GFP

Figure 14 p27kip1 binds miR-223.

A, Expression of miR-223 and p27 protein using the anti-EGFP or the anti-p27 antibodies (Ab#Cl57), in lysates and RIP from MDA-MB-231-miR-223 cells transfected with the indicated p27 constructs and immunoprecipitated using an anti-EGFP or control IgG antibodies, as indicated. In the lower graph qRT-PCR analyses, evaluating miR-223 binding to p27WT or mutant proteins expressed as fold enrichment respect to miR-223 binding to EGFP transfected cells. **B**, Expression of miR-223 and p27 protein using the anti-EGFP antibody in lysates and IP from MDA-MB-231 cells transfected with miR-223 and the indicated p27 constructs. **C**, Expression of miR-223 and p27 protein using the anti-EGFP antibody in lysates and IP from HT-1080 cells transfected with miR-223 and the indicated p27 constructs.

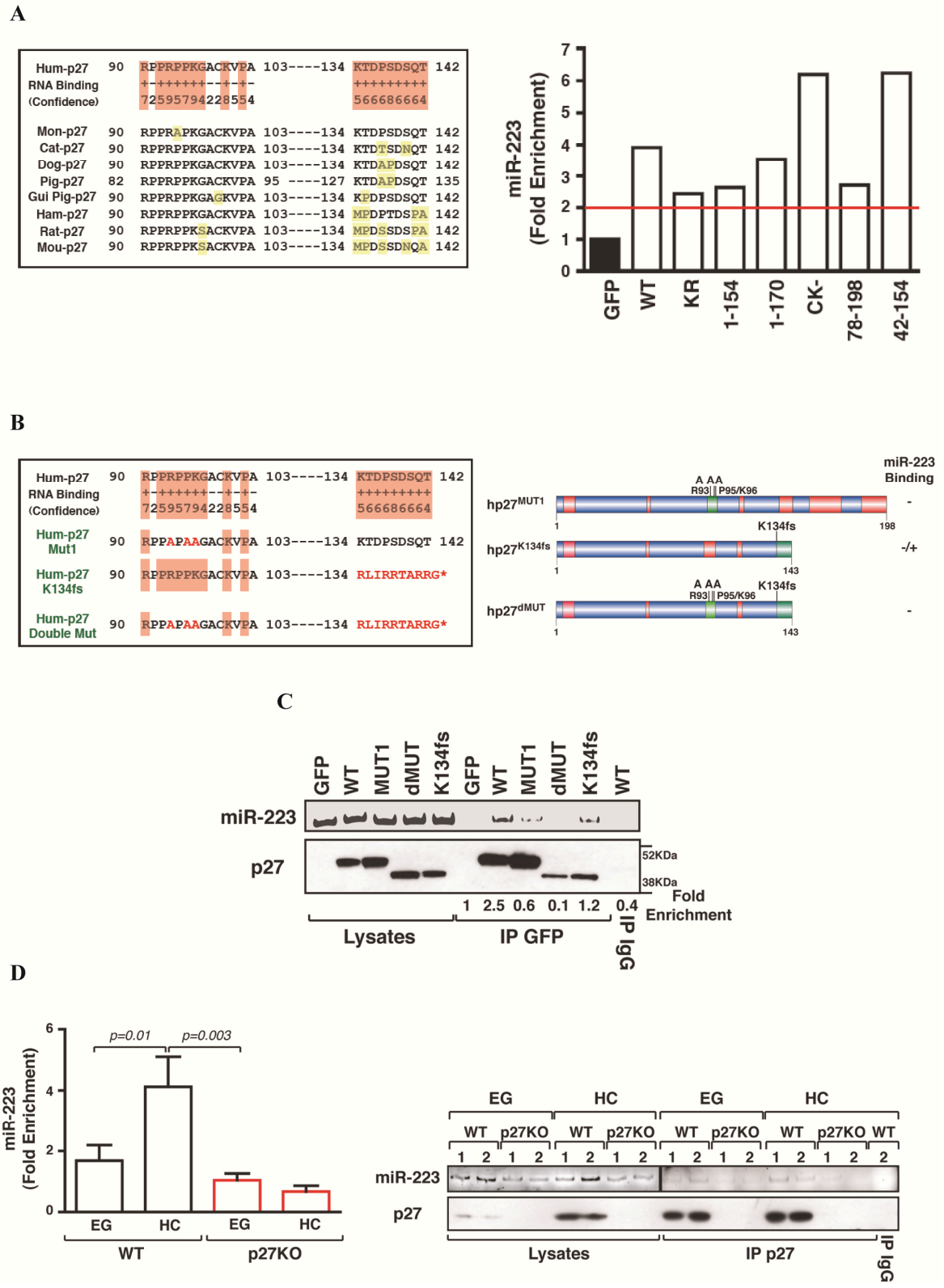
A
Hum-p27 90 RPPRPPKGACKVPA 103----134 KTDPSDSQT 142
RNA Binding +-+++++++--+-+- +++++++++
(Confidence) 725957942285 54 566686664
Mon-p27 90 RPPRAPKGACKVPA 103----134 KTDPSDSQT 142
Cat-p27 90 RPPRPPKGACKVPA 103----134 KTDTSDNQT 142
Dog-p27 90 RPPRPPKGACKVPA 103----134 KTDAPDSQT 142
Pig-p27 82 RPPRPPKGACKVPA 95 ----127 KTDAPDSQT 135
Gui Pig-p27 90 RPPRPPKGAGKVPA 103----134 KPDPSDSQT 142
Ham-p27 90 RPPRPPKGACKVPA 103----134 MPDPTDSPA 142
Rat-p27 90 RPPRPPKSACKVPA 103----134 MPDSSDSPA 142
Mou-p27 90 RPPRPPKSACKVPA 103----134 MPDSSDNQA 142
miR-223 (Fold Enrichment)
0 1 2 3 4 5 6 7
GFP WT KR 1-154 1-170 CK- 78-198 42-154
B
Hum-p27 90 RPPRPPKGACKVPA 103----134 KTDPSDSQT 142
RNA Binding +-+++++++--+-+- +++++++++
(Confidence) 725957942285 54 566686664
Hum-p27 Mut1 90 RPPAPAAGACKVPA 103----134 KTDPSDSQT 142
Hum-p27 K134fs 90 RPPRPPKGACKVPA 103----134 RLIRRTARRG*
Hum-p27 Double Mut 90 RPPAPAAGACKVPA 103----134 RLIRRTARRG*
miR-223 Binding
hp27MUT1 A AA R93 P95/K96 1 198 -
hp27K134fs K134fs 1 143 -/+
hp27dMUT A AA R93 P95/K96 K134fs 1 143 -
C
GFP WT MUT1 dMUT K134fs GFP WT MUT1 dMUT K134fs WT
miR-223
p27
52KDa
38KDa
1 2.5 0.6 0.1 1.2 0.4
Fold Enrichment
Lysates
IP GFP
IP IgG
D
miR-223 (Fold Enrichment)
p=0.01 p=0.003
0 2 4 6
EG HC EG HC
WT p27KO
EG HC EG HC
WT p27KO WT p27KO WT p27KO WT p27KO WT
1 2 1 2 1 2 1 2 1 2 1 2 1 2 1 2 2
miR-223
p27
Lysates
IP p27
IP IgG

Figure 15 miR-223 is bound to p27 through a conserved region.

A, Comparison of p27 protein sequence among mammals in the putative miR-223 binding region. The aminoacids predicted to bind RNA in human p27 using the BindN resource are highlighted in red (score 1 to 9, with 1=lowest and 9=highest value). Aminoacid substitutions in the different mammals are highlighted in yellow. The graph on the right reports miR-223 binding to $p27^{WT}$ or mutant proteins, expressed as fold enrichment respect to miR-223 binding in GFP transfected HT-1080 cells. **B**, Schematic representation of the 3 mutants used to precisely map the miR-223 binding domain in p27. The $p27^{MUT1}$ construct carries three substitutions (R93A, P95A and K95A) that completely alter the RNA binding domain between aa 90 and 103 as predicted using the BindN resource. The $p27^{K134fs}$ construct carries one base deletion (A420) resulting in the frame shift of the protein from K134 and in the generation of a truncated protein of 143 aa that lost the RNA binding domain between aa 134 and 143 (the alternate frame is reported in red). The $p27^{dMUT}$ (double mutant) construct carries both RNA binding domains deletions. **C**, Expression of miR-223 and p27 protein using the anti-p27 antibodies (Ab#Cl57), in lysates and RIP from MDA-MB-231-miR-223 cells transfected with the indicated p27 constructs and immunoprecipitated using an anti-EGFP or control IgG antibodies, as indicated. The fold enrichment value (calculated as in A) is reported under the blot. **D**, qRT-PCR analyses evaluating miR-223 binding to endogenous p27 protein expressed as fold enrichment respect to miR-223 binding to control IgG in WT and p27KO cells, cultured in exponential growth (EG) or at high confluence (HC). On the right, expression of miR-223 (upper panel) and p27 protein (lower panel) is reported. Different MEF preparations (1 and 2) are indicated. p values were obtained by unpaired student t-test, using either Excel or Prism software.

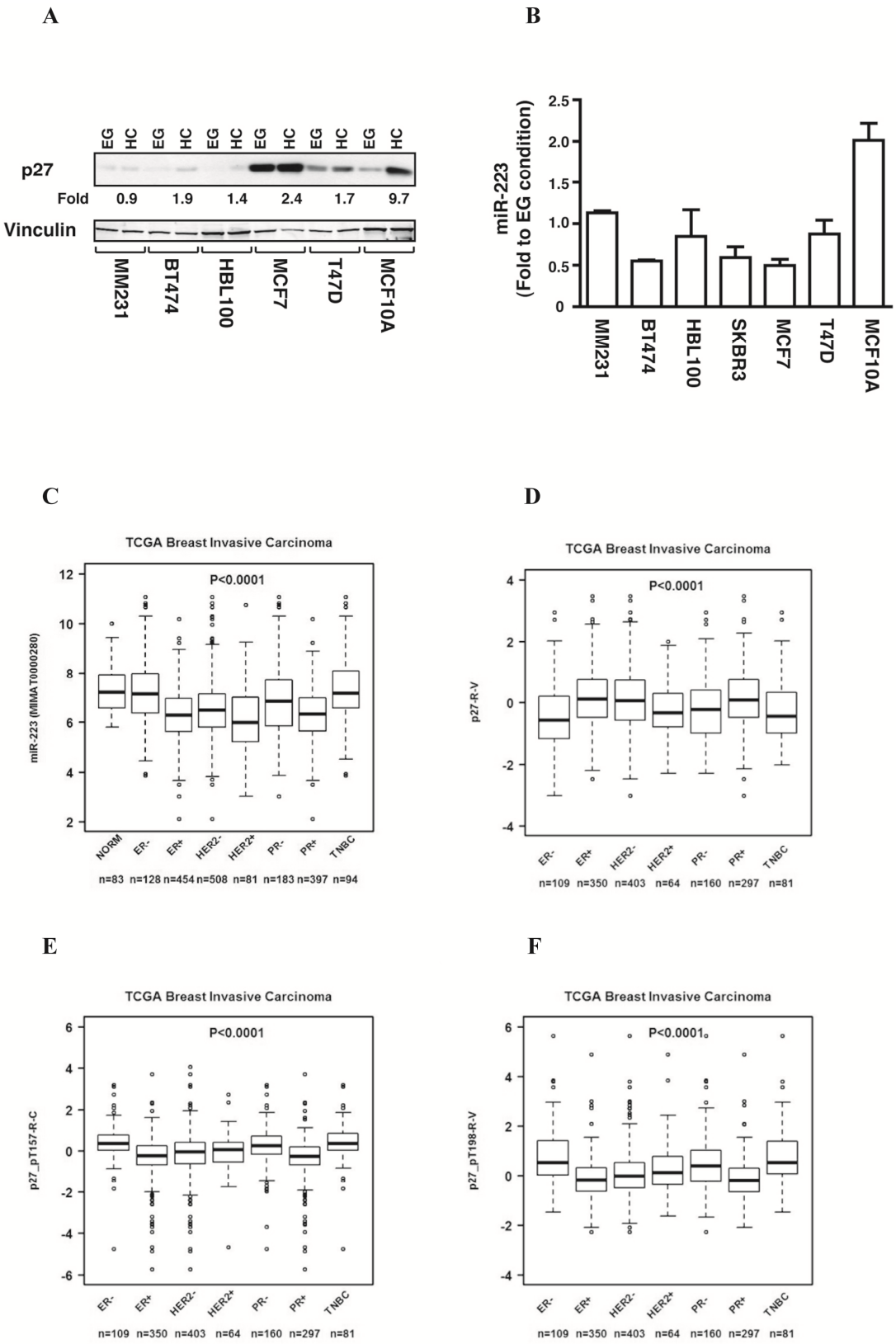
A
EG HC EG HC EG HC EG HC EG HC EG HC
p27
Fold 0.9 1.9 1.4 2.4 1.7 9.7
Vinculin
MM231 BT474 HBL100 MCF7 T47D MCF10A
B
miR-223 (Fold to EG condition)
2.5 2.0 1.5 1.0 0.5 0
MM231 BT474 HBL100 SKBR3 MCF7 T47D MCF10A
C
TCGA Breast Invasive Carcinoma
P<0.0001
miR-223 (MIMAT0000280)
NORM ER- ER+ HER2- HER2+ PR- PR+ TNBC
n=83 n=128 n=454 n=508 n=81 n=183 n=397 n=94
D
TCGA Breast Invasive Carcinoma
P<0.0001
p27-R-V
ER- ER+ HER2- HER2+ PR- PR+ TNBC
n=109 n=350 n=403 n=64 n=160 n=297 n=81
E
TCGA Breast Invasive Carcinoma
P<0.0001
p27_pT157-R-C
ER- ER+ HER2- HER2+ PR- PR+ TNBC
n=109 n=350 n=403 n=64 n=160 n=297 n=81
F
TCGA Breast Invasive Carcinoma
P<0.0001
p27_pT198-R-V
ER- ER+ HER2- HER2+ PR- PR+ TNBC
n=109 n=350 n=403 n=64 n=160 n=297 n=81

Figure 16 p27-miR-223 axis is deregulated in breast cancer.

A, Western blot analysis of p27 expression in breast cancer cell lines, harvested in exponential growth (EG) or at high confluence (HC). Increase of p27 expression in cells grown at HC, expressed as fold increase respect to EG condition, is reported in the figure. Vinculin was used as loading control. **B**, miR-223 expression in the indicated breast cancer cell lines grown at HC. Data are expressed as fold increase of miR-223 levels in HC respect to EG. Expression of miR-223 (**C**), p27 (**D**), p27 pT157 (**E**) and p27 pT198 (**F**) in the TGCA dataset, evaluated by microarray analyses (**C**) or RPPA (**D-F**).

By looking at the expression and phosphorylation of p27 in the same data set (403 cancer specimens analyzed by reverse-phase protein array, RPPA) (166) we showed that, although p27 levels were higher in ER+ and PR+ breast cancers (Figure 16D), its phosphorylation on T157 (Figure 16E) and T198 (Figure 16F) was higher in TNBC. Interestingly, phosphorylation on T157 but not on T198 significantly correlated with miR-223 expression in TNBC (Figure 17A). T198 phosphorylation has been linked to p27 degradation (163) while T157 phosphorylation has been linked to p27 displacement in the cytoplasm (167), suggesting that the latter could participate in the regulation of miR-223 binding. To this aim we generated a non-phosphorylable T157 mutant (p27T157A) and a pseudo phosphorylated mutant (p27T157D) to be tested in RIP assays (Figure 17B). Data showed that p27 ability to bind miR-223 paralleled the levels of T157 phosphorylation, with the p27T157D mutant displaying the greatest ability (Figure 17B and C), thus providing an explanation for the positive correlation observed in breast cancers (Figure 17A).

A

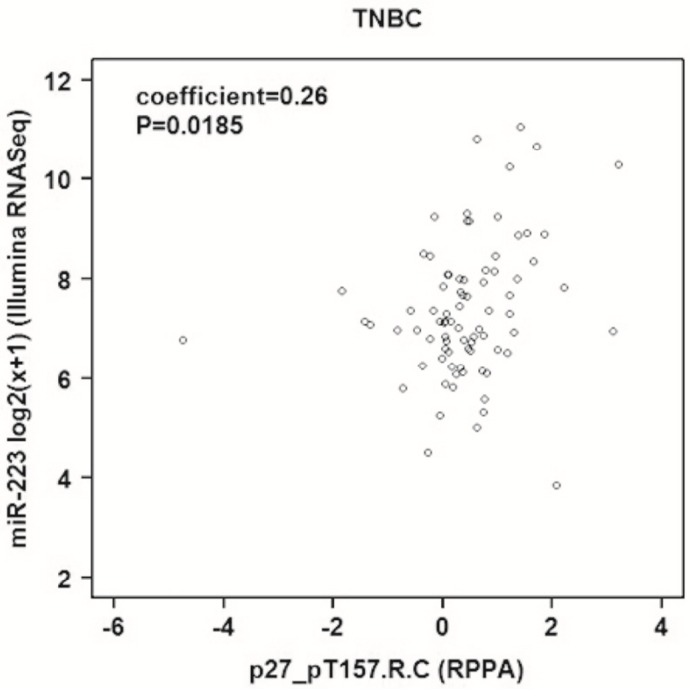
TNBC
coefficient=0.26
P=0.0185
miR-223 log2(x+1) (Illumina RNASeq)
p27_pT157.R.C (RPPA)
12
10
8
6
4
2
-6
-4
-2
0
2
4

B

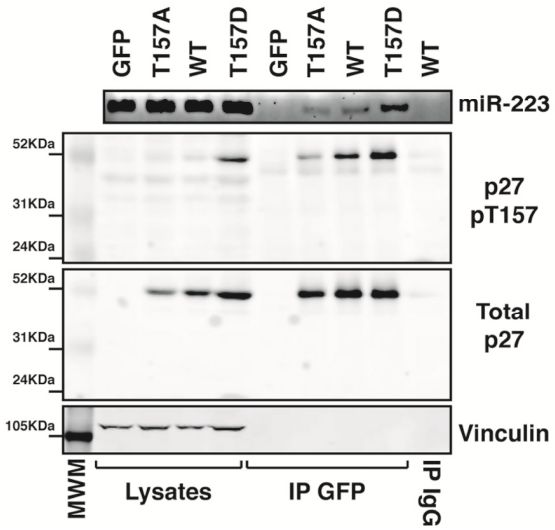
GFP
T157A
WT
T157D
GFP
T157A
WT
T157D
WT
miR-223
52KDa
31KDa
24KDa
p27
pT157
52KDa
31KDa
24KDa
Total
p27
105KDa
Vinculin
MWM
Lysates
IP GFP
IP IgG

C

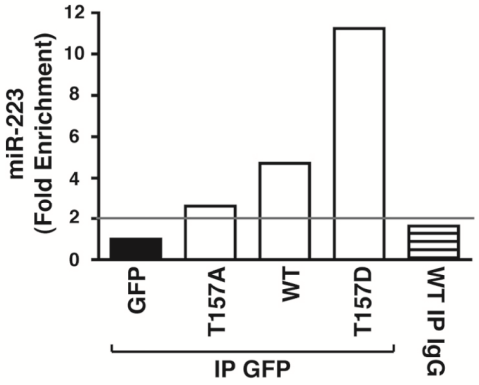
miR-223
(Fold Enrichment)
12
10
8
6
4
2
0
GFP
T157A
WT
T157D
WT IP IgG
IP GFP

Figure 17 The cytoplasmic displacement of p27-pT157 positively correlates with miR-223 expression and binding.

A, Correlation between miR-223 and p27-pT157 expression in the TCGA breast cancer dataset, using the Spearman's correlation test. **B**, Expression of miR-223, p27 T157 and p27 in lysates and RIP from MDA-MB-231-miR-223 cells, transfected with the indicated EGFP-p27 constructs and immunoprecipitated using an anti-EGFP or control IgG antibodies, as indicated. **C**, miR-223 expression in RIP described in (B), evaluating binding to p27WT or mutant proteins and expressed as fold enrichment respect to miR-223 binding in EGFP transfected cells.

Discussion

An increasing number of evidences indicates that miRs control cell cycle progression by direct targeting of critical modulators, such as cyclins, CDKs and CDK inhibitors (50-54). The crucial cell cycle checkpoints are tightly controlled at several levels by different miRs (53). For example, the mir-15a-16-1 cluster induces cell cycle arrest by targeting critical cell cycle regulators, such as CDK1, CDK2 and CDK6, as well as cyclins (D1, D3 and E1) (168). Indeed, these and other promoters of the cell cycle, such as cyclins (45) and cell division cycle phosphatases, like CDC25A (169), are also known to be targeted by other miRs to inhibit the cell cycle and different reports show that these miRs are downregulated or lost in tumor cells (53, 170).

Conversely, cancer cells frequently up-regulate the expression of miRs that target inhibitors of cell cycle progression. For example, pRB and family members p107 and p130 are targets of miRs found to be upregulated in certain cancers (32, 171).

One of the best characterized link between cell cycle repressors and miRs is represented by the role of miR-221/222 in the regulation of p27 expression (50, 57). It has been demonstrated that in cells exposed to mitogenic stimuli, when p27 protein expression decreases (58, 59) miR 221/222 expression increases, determining an amplification of the pro-mitogenic stimuli that ultimately favors the entrance in S phase (53, 57).

The role of miRs in the control of cell cycle progression is intimately correlated with the alteration of cell proliferation and the relevance of cell cycle regulation induced by miRs in cancer is well documented in several cancer tissues (47-49).

During this PhD project we studied the role of p27 in the regulation of cell cycle-related miRs and we uncovered a novel role for p27 in the control of cell cycle arrest, mediated by the control of miR expression and stability.

To approach this issue, we used wild type and p27KO cells harvested in different phases of the cell cycle and identified the miRs regulated by p27 during the G1 to S phase transition. We found that miR-223 was the most up-regulated miR in G1 arrested MEFs. The major increase in miR-223 levels was achieved when the G1 arrest was imposed by contact inhibition occurring in highly confluent cells. Interestingly, in the absence of p27 miR-223 levels were strongly reduced and unaffected by cell cycle arrest.

Contact inhibition occurs in normal cells and is lost in cancer cells, allowing for uncontrolled growth even after that the confluence is reached (132, 136).

p27 is a master regulator of G1 arrest following contact inhibition and its protein expression is highly increased when cells reach high confluence (59, 68, 143, 153, 154). Nevertheless,

the molecular mechanisms that drive contact inhibition through the up-regulation of p27 expression are still unclear. Generally, it has been observed that widespread gene expression changes occur when cells enter quiescence, including both repression and activation of genes (64-67). Several important regulators of this process have been described, particularly the MYC and E2F families of transcription factors, that coordinate cell cycle re-entry and repress cell cycle genes during quiescence (66, 172, 173). In the last few years, also regulation of miR expression has been correlated with the quiescent state (174). Four microRNAs were upregulated and over 100 microRNAs were downregulated as T98G glioblastoma cells progress from quiescence into the proliferative status (174). Recently, it was demonstrated that the quiescence state induced by contact inhibition promotes the down-regulation of miR-29 and the consequent release from repression of its targets, contributing to the reinforcement of the concept that contact inhibition is an active state (71).

We thus decided to pursue the study of our interesting results, by investigating by which molecular mechanisms p27 expression could trigger miR-223 up-regulation when high cellular confluence was reached. First of all, we decided to test whether cell-cell contacts were necessary to sustain the expression of miR-223. Our results clearly demonstrated that the establishment of stable cell-cell contacts was the initiating event that led to a sustained expression of miR-223 and this in turn required the presence of p27.

It is known that regulation of miRs expression can be achieved either by acting on miR transcription (175, 176) or by post-transcriptional mechanisms (72, 177). Interestingly, we found that the impairment of miR transcription did not affect miR-223 levels in the presence of p27, while in p27KO cells miR-223 levels dramatically dropped (Figure 8A-C), indicating that p27 mediated miR-223 stability through a post-transcriptional mechanism. Strikingly, using a microRNA *in vitro* degradation assay, we demonstrated that p27 was able to specifically lengthen the half-life of a synthetic miR-223 oligo, suggesting that p27 stabilizes and protects miR-223 from degradation (Figure 13A and B). These results were of particular interest considering that, in the last few years, increasing attention has been focusing on the mechanisms that regulate miR stability (72, 176, 177). miRs are found to be generally stable and mature miRs persist for hours, or even days, after their production is arrested (18-20). However, although crucial for the regulation of steady-state miR levels, little has been uncovered about the regulation of miR half-life and stability in the cell, following processing. Although >10 fold more stable than mRNA (the median half-life of which is 10 h), some miRs, such as miR-125b, are more persistent than others (19).

Our results therefore added a new piece of knowledge in the understanding of the post-transcriptional mechanisms that control miR stability.

Moreover, using RNA immunoprecipitation assay, we proved that miR-223 is physically bound to p27 (Figure 13C, 14A-D) and that this interaction is conserved from mouse to human (Figure 13C, 14A and E). We identified two possible miR-223 binding motifs (RNA-BM) in human p27: one between aa 90-103 and the second between aa 134-142. It is intriguing to note that two point mutations within the first RNA-BM (P95S and K96Q) have been found in MEN syndromes (178), thus strongly supporting the idea that this binding is relevant in cancer. The K96Q substitution, predicted to profoundly alter the miR-223 binding motif in p27 (by BindN software analysis) is also associated with the presence of breast cancer in MEN patients (178). More interestingly, two frame shifts mutations (K134fs and P137fs) found in luminal A breast cancer (reviewed in ref. 165) completely disrupt the second RNA-BM, reinforcing the potential significance of our findings in breast cancer onset and/or progression.

In this PhD project, we demonstrated that contact inhibition is an active state in which the coupled increase of p27 and miR-223 is crucial to lead to G1 arrest. Our data convincingly establish that p27 regulates miR-223 stabilization and protects from degradation through a physical interaction.

However, our data did not explain the increase in miR-223 transcription induced by cell-cell contact in both WT and p27KO cells. We thus investigated how cell confluence could trigger miR-223 transcription and our results demonstrated that p27 regulates miR-223 also by another mechanism, related to its ability to inhibit pRB phosphorylation by CDKs, thus eventually blocking E2F1 activity. We discovered an auto regulatory feedback loop between E2F1 and miR-223, in which E2F1 repressed the miR-223 promoter and miR-223 downregulates E2F1 expression (Figure 9B, 10A and B).

Importantly, this E2F1-miR-223 feedback loop plays a role in the regulation of cell cycle exit since miR-223 silencing in p27WT cells rescues the G1 arrest imposed by contact inhibition (Figure 11A). Conversely, miR-223 overexpression resulted in a delayed S phase entrance (Figure 11B and C).

Our data, showing that in p27KO cells contact inhibition failed to properly downregulate E2F1 (Figure 9C), add new elements to the mechanism by which this crucial transcription factor is regulated and open interesting lines of future investigation. Our results are in accord with the phenotypes of p27 (161) and miR-223 (83) knock-out animals, both presenting

features of hyper proliferation. Future investigation will establish whether the mechanism highlighted here plays a role in the physiology/pathology of lymphoid organs, particularly enlarged in both p27 and miR-223 knock-out mice (161, 83).

In summary, the present PhD thesis shows that contact inhibition induces accumulation of p27 and this in turn impinges on miR-223 expression in a dual manner. Nuclear p27 counteracts E2F1 activity by impairing RB phosphorylation, thereby increasing miR-223 transcription. Cytoplasmic p27 directly binds mature miR-223 increasing its stability.

This work uncovers a new function of p27 that through a physical interaction with miR-223 regulates its stability to enhance the proliferative arrest following contact inhibition.

Future investigation will address if and how post-translational modifications of p27 following contact inhibition modulate its ability to bind and stabilize miR-223. It is conceivable that one of these modifications might be the phosphorylation of p27 on T157 that correlates with miR-223 levels in TNBC and significantly increases the binding of p27 to miR-223 *in vitro*.

In conclusion, we highlight a new pathway that participates to the control of cell proliferation both *in vitro* and *in vivo* and represents a promising field of future investigation for cancer research and anti-cancer therapeutics, especially in breast cancer.

Materials and Methods

Cell culture

Primary wild type (WT) and p27 knock-out (p27KO) mouse embryo fibroblasts (MEFs) were prepared from embryos at day 13.5, as previously described (179).

Primary MEFs (at least 3 different preparations/genotype) were frozen at passage 1 and used in all subsequent experiments between passage 2 and 4, without significant differences. The correct genotype of WT, p27KO cells was determined by PCR, as described (179). 3T3 fibroblasts were obtained from primary MEFs following the 3T3 immortalization protocol, as described elsewhere (144). MEFs and 3T3 fibroblasts were cultured in Dulbecco modified Eagle medium (DMEM) supplemented with 10% fetal bovine serum (FBS) (Sigma).

MDA-MB-231, HT-1080, BT-474, HBL-100, SK-BR-3, MCF-7, T47-D, MCF-10A and 293T-17 cell lines were obtained from ATCC (LGC Standards). 293FT cell line was purchased from Life Technologies (Invitrogen). Cells were all cultured in DMEM supplemented with 10% FBS, except for MCF-10A cells, cultured in Mammary Epithelial Cell Growth Medium supplemented with bullet kit (Promo Cell).

mmu-miR-expression profile and qRT-PCR

Total RNA (5 μg) was reverse transcribed using biotin end-labeled random octamer oligonucleotide primers. Hybridization of biotin-labeled complementary DNA was performed using a custom miR microarray chip (OSU-CCC Human and Mouse MicroRNA Microarray Version 4.0) which contains 1,600 miR oligo probes derived from 474 human and 373 mouse miR genes and printed in duplicates. The hybridized chips were washed and processed to detect biotin-containing transcripts by streptavidin–Alexa647 conjugate, scanned and quantitated using an Axon 4000B scanner (Axon Instruments, Downingtown, PA) and the GenePix 6.0 software (Axon Instruments, Downingtown, PA). Three replicates were tested for each sample. Average values of the replicate spots of each miR were background subtracted, normalized, and further analyzed. Normalization was performed using the global median method. We selected the miRs measured as present in at least as many samples as the smallest class in the data set (50%). Absent calls were thresholded to 6.2 (log2 scale) before statistical analysis, representing the average minimum intensity level detectable in the system. Differentially expressed miRs were identified using the Class Comparison Analysis of BRB tools version 3.6.0 (http://linus.nci.nih.gov/BRB-ArrayTools.html). The criterion for inclusion of a gene in the gene list is a p-value less than

0.05. The miR expression data have been submitted to the Gene Expression Omnibus (GEO) with accession number GSE 45538.

RNA from exponentially growing (EG), G1-blocked (G1) and S-phase (S) p27WT and p27KO MEFs used for the array data were further used for miR validation by qRT-PCR.

Vectors

Retroviral vectors (murine stem cell virus retroviral vectors, MSCV; Clontech) or EGFP-tagged vectors encoding for human p27WT, mutant p27CK- (R30, L32, F62, F64 in Alanine), mutant p27KR (K165, R166 in Alanine), mutant $p27T157^{A}$ (T157 in Alanine) or $p27T157^{D}$ (T157 in Aspartate) in were produced by site directed mutagenesis using a dedicate kit (Stratagene) as described elsewhere (163). The EGFP-tagged p27 deletion mutants were previously described (179) or generated by PCR starting from human p27 cDNA using the following primers:

p27 P 1 FW: 5'-GGATCCCATATGTCAAACGTGCGAGTG-3'

p27 P 26 FW: 5'-GGATCCCATATGCCCTCGGCCTGCAGGAAC-3'

p27 P 42 FW : 5'-GGATCCCATATGACCCGGGACTTGGAGAA-3'

p27 P 78 FW : 5'-GGATCCCATATGGAGGTGGAGAAGGGCAGC-3'

p27 P 85 RV: 5'- GGATTCCTCGAGGGGCAAGCTGCCCTTCTC-3'

p27 P 154 RV: 5'-GGATCCCTCGAGTCGCTTCCTTATTCCTGC-3'

p27 P 170 RV: 5'-GGATCCCTCGAGTGTTCTGTTGGCTCTTTT-3'

p27 P 198 RV: 5'-GGATCCCTCGAGTTACGTTTGACGTCTTCT-3'

Lentiviruses expressing miR-223 were produced in 293-FT cells (Invitrogen), by calcium phosphate transfection. To this purpose, the System Biosciences (SBI, USA) microRNA Precursor Constructs were used, containing expression of the specific microRNA, encoding also for the puromycin resistance for simple identification and monitoring of cells positive for transduction. In particular, MDA-MB-231 and HT-1080 cell lines were transduced with lentiviruses expressing precursor of miR-223 and transduced cells were selected using 1.5 µg/ml puromycin. Production of bacterial recombinant p27 protein was performed as previously described (163). Briefly, p27WT cDNA was cloned in the pQE-30 vector (Qiagen). Escherichia coli (M15) cells were transformed with the expression plasmid to produce recombinant proteins containing His-tag at the N-terminus. Proteins were subsequently purified with Ni-nitrilotriaceticacid (NiNTA) resin (Qiagen).

Cell Treatment and qRT-PCR

MEFs were harvested at several culture conditions: exponential growth (EG), serum starvation (ST), release in complete medium (10% FBS) for 13-15 hours (R13, R15), high confluence (HC) and high confluence followed by serum starvation (HC ST).

In the conditioned media experiment, exponentially growing p27WT MEF were grown in conditioned media harvested from exponentially growing (EG) or highly confluent (HC) MEFs. RNA was then extracted after 24 hrs for qRT-PCR analysis. In the cell-splitting experiment, p27WT and p27KO MEFs were cultured in HC condition and then replated at high (HC, $4x10^4$ cells/cm^2 dish) or low (LC, $1x10^4$ cells/cm^2) confluence. RNA was then extracted after 4, 8 and 24 hrs for qRT-PCR analysis. In the EGTA experiment, MEFs grown at HC were treated with 5mM EGTA. RNA from treated and untreated cells was extracted after 1 hr for qRT-PCR analysis. In the Actinomycin D experiment, MEFs grown at HC were treated with Actinomycin D (5 mg/ml, Sigma-Aldrich). RNA was extracted at each indicated time for qRT-PCR analysis. In the α-amanitin experiment, MEFs grown at HC were treated with α-amanitin (20μg/ml, as described in Chen et al., 2012). RNA was extracted at each indicated time for qRT-PCR analysis. In the experiment of miR-223 exogenous expression, MEFs were transduced with lentiviral vectors encoding for miR-223 and 72 hrs later cells were cultured at HC and then treated with 5mM EGTA for 1 hour. In the experiment of miR-223 expression in 3T3 fibroblasts, 3T3 p27KO cells were clones were transduced with retroviral vectors encoding for p27WT, p27CK- and p27KR proteins. Exponentially growing fibroblasts were then harvested for RNA preparation and qRT-PCR analysis. RNA was extracted using Trizol reagent (Invitrogen) and retro-transcribed using the TaqMan MicroRNA Reverse Transcription Kit (Applied Biosystems). MicroRNAs expression levels were quantified by qRT-PCR, using the Single Tube TaqMan microRNA Assay and the Universal Master Mix (Applied Biosystems). Normalization of the data was performed using the U6 snRNA expression. Reverse Transcriptase reactions and Real-Time PCR were performed according to the manufacturers' instructions. qRT-PCR reactions were run in the MyiQ2 Two Color Real-time PCR Detection System (Biorad). Comparative real-time PCR was performed in triplicate, including no-template controls. Relative expression was calculated using the comparative $2^{\wedge-\Delta Ct}$ method. In the pri-miR-223 experiment, RNA from EG or HC MEFs was retro-transcribed with AMV Reverse transcriptase to obtain cDNAs,

according to provider's instruction, (Promega). Absolute quantification of mouse pri-miR-223 was evaluated by qRT-PCR using SYBR Green dye-containing reaction buffer (GoTaq qPCR 2x Master Mix, Promega). Standard curves (10-fold dilution from 10^{1} to 10^{-4} attomoles) were prepared for both pri-miR-223 and housekeeping genes. The incorporation of the SYBR Green dye into the PCR products was monitored in real time using the MyiQ2 Two Color Real-time PCR Detection System (Biorad). Ct values were converted into attomoles. Then normalized pri-miR-223 value was obtained by using at least two different housekeeping genes (GAPDH, GUSB). The following primers (Sigma) were used:

mouse pri-miR-223 FW: 5'-TCCAGTTGCACATCTTCCAG-3'

mouse pri-miR-223 RV: 5'-TGTAGGCAGCAGGCTATGTG-3'

mouse GusB FW: 5'-CTCTGGTGGCCTTACCTGAT-3'

mouse GusB RV: 5'-CAGTTGTTGTCACCTTCACCTC-3'

mouse GAPDH FW: 5'-TGAGGACCAGGTTGTCTCCT-3'

mouse GAPDH RV 5'-CCCTGTTGCTGTAGCCGTAT-3'

Luciferase assay and mutagenesis

A 5'-flanking fragment of mouse pri-miR-223 (AK036748, according to 77) from position –758 to +23 relative to the transcription start site (+1) was amplified from mouse genomic DNA (C57/BL6 mouse), using specific primers carrying restriction endonuclease sequences XhoI (in the sense primer) and Hind III (in the antisense primer). PCR product was digested with Xho I and Hind III, unidirectionally subcloned into the promoter-less pGL3 basic vector (Promega) creating miR-223 promoter full length (FL).

Putative binding sites for E2F1 transcription factor were explored by conducting the Transcription Element Search System (http://www.cbil.upenn.edu/tess/index.html) and by PROMO 3.0 (alggen.lsi.upc.es/recerca/menu_recerca.html).

For the E2F1 deleted fragments (E2F1Del) a sense primer downstream of the two putative E2F1 binding sites with restriction endonuclease sites XhoI was used and cloned as described for FL vector.

mmu-miR-223 promoter FL F: 5ACGCTCGAGGGTGCTGTTACAAAGATAAGGCAAA-3'

mmu-miR-223 promoter FL R: 5'-ACGAAGCTTAAGTGGTGCCTTTGTCTTGG-3'

mmu-miR-223 promoter E2F1Del F: 5'-ACGCTCGAGGGGAAGTCAGTGTTTTTGGAG-3'

For the point mutations of E2F1 binding sites site-directed mutagenesis of the FL vector was performed using the QuikChange Site-Directed Mutagenesis Kit (Stratagene) according to the manufacturer's instructions using the following primers:

mmu-miR-223 promoter E2F1 Mut 1 F:
5'-GCTCTGATATTTAAAGATCTCAATTGCTCTAGGG-3'
mmu-miR-223 promoter E2F1 Mut 1 R:
5'-CCCTAGAGCAATTGAGATCTTTAAATATCAGAGC-3'
mmu-miR-223 promoter E2F1 Mut 2 F:
5'-GTACTTCCTGCTTCACTCTGTAGCATG-3'
mmu-miR-223 promoter E2F1 Mut 2 R:
5' -CATGCTACAGAGTGAAGCAGGAAGTAC-3'

E2F1 Mut 3 vector was generated using E2F1 Mut 1 as template and mmu-miR-223 promoter E2F1 Mut 2 as primers for mutagenesis assay performed as described above.
For the luciferase assays, MEFs were cotransfected with 15µg of one of the reporter constructs (ppri-mir-223-full length, ppri-mir-223-E2F1-del or pGL3 basic vector) and 2.5µg of pTK-RL vector (internal control) using Lipofectamine reagent (Invitrogen) according to manufacturer's recommendations.
After transfection, cells were plated at EG and HC and 24 hrs later, cell lysates were assayed for luciferase activity using the Dual-Luciferase reporter assay system (Promega). Values were normalized using Renilla luciferase.

BrdU assay and FACS analysis

For BrdU incorporation assay, MEFs were transfected with a synthetic miR-223 inhibitor (Life Technologies) using oligofectamine reagent (Life Technologies).
Cells were then harvested at EG or at HC from 60mm dishes (BD, Falcon) containing coverslips (Menzel-Glaser, 12 mm) and were incubated for 3 hours with 10 µM BrdU (Roche). WT and p27KO MEF overexpressing miR-223 or control empty vector were starved and grown at high confluence (HC-ST) and then released in complete medium for 13, 16, 18 hours (R-13, R-16, R-18). Cells were then fixed in 4% paraformaldehyde (PFA) in PBS at room temperature (RT) and permeabilized in HCl 1,5 N for 30 minutes at 37°C. Coverslips were then washed 2 times in Borate Buffer 0.1 M pH 8.5 and 2 times in PBS.

Incubation with primary antibody anti-BrdU (Roche) was performed 1 hour at 37°C, and samples were washed in PBS and incubated with secondary antibody (anti-mouse Alexa Fluor488-conjugated, Invitrogen) for 1 hour at RT. Finally, nuclear staining with propidium iodide 3 µg/ml + RNase 100 µg/ml for 30 minutes at RT was performed and coverslips were mounted on glass slides with Mowiol 488 (Calbiochem).

Cell cycle distribution was analyzed by flow cytometry (FACS). WT MEF overexpressing miR-223 or control empty vector were starved and grown at high confluence (HC-ST) and then released in complete medium for 13, 16, 18 hours (R-13, R-16, R-18). Cells were then collected, fixed in ice-cold 70% ethanol, washed in PBS 1x and resuspended in propidium iodide staining solution (50 µg/ml propidium iodide and 100 µg/ml RNase A, in PBS 1X). Stained cells were subjected to FACS analysis with a FACScan or a FACSCalibur instrument (BD Biosciences). Distribution of cells in G1, S and G2/M phases of the cell cycle was calculated using the WinMDI2.8 software.

Immunofluorescence analysis

For immunofluorescence analysis EG, ST and HC MEFs and EG 3T3 p27KO fibroblasts (+$p27^{WT}$, +$p27^{CK-}$, +$p27^{KR}$) were harvested from 60mm dishes (BD Falcon) containing coversplips (Menzel-Glaser, 12 mm) and fixed in phosphate-buffered saline (PBS)–4% paraformaldehyde (PFA) at room temperature (RT), permeabilized in PBS–0.2% Triton X-100, and blocked in PBS–1% bovine serum albumin (BSA). Incubation with primary anti-p27 antibody (sc-528, Santa Cruz) was performed overnight at 4°C in PBS–1% BSA, then samples were washed in PBS and incubated with secondary antibodies (Alexa Fluor 488-conjugated anti-rabbit antibody, Invitrogen) for 1h at RT. Antibody incubation was followed by nuclear staining with propidium iodide solution (propidium iodide 3 µg/ml + 100 µg/ml RNase in PBS) for 30 min at RT. Stained cells were observed using a confocal laser-scanning microscope (TSP2 Leica) interfaced with a Leica DMIRE2 fluorescent microscope.

In vitro microRNA degradation assay

The *in vitro* microRNA degradation assay was essentially performed as described elsewhere (180). Proteins from p27KO MEF cells were extracted at 4°C using degradation buffer (50mM Tris–HCl, pH 8.0, 10mM MgCl2, 75mM KCl, 5mM DTT, 10mM ascorbic acid and protease inhibitor cocktail, Roche) and after 2 cycles of freeze

and thaw lysates were centrifuged to pellet debris. 5µg of RNA oligos hsa-miR-223, hsa-miR1 or control miR (Sigma Aldrich) were added to 100µg of protein lysate and incubated at 25°C for 90 and 120 min with the addition of 1µg/µl recombinant p27 protein (1µg/sample) or degradation buffer as a control. At indicated times, each reaction was split in two aliquots: one aliquot for evaluation of oligo RNA levels, to which 2x loading dye (8M urea, 20mM Tris–HCl pH 8.0, 1mM EDTA, pH 8.0, 0.025% xylene cyanol FF and 0.025% bromophenol blue) was added; the other aliquot for evaluation of protein expression, to which 2x Laemli buffer was added. Samples were denatured at 95°C for 5 min. Oligo RNAs were separated on a 15% denaturing polyacrylamide gel, while total proteins were separated in 4-20% SDS-PAGE (Criterion Precast Gel, Biorad).

RNA immunoprecipitation

For prediction of RNA-binding residues of p27 protein, a search using BindN web-tool (http://bioinfo.ggc.org/bindn/) as described (181) was conducted using human and mouse p27 amino acid sequence as inputs.

Stable cell lines expressing miR-223 (MDA-MB-231, HT-1080) described before, were transfected with 10µg of pEGFP-p27 expression vectors using FuGENE HD transfection reagent (Promega). 48 hours later cells were harvested for protein extraction.

RNA immunoprecipitation assay (RIP) was performed essentially as previously described (182). To extract total proteins cells were scraped on ice using cold RIPA lysis buffer (150mM NaCl, 50mM Tris HCl pH 8.0, 1% NP40, 0.5% sodium deoxycholate, 0.1% SDS) plus a protease inhibitor cocktail (Complete™, Roche) and supplemented with 1 mM Na3VO4 (SIGMA), 1 mM DTT (SIGMA) and 100U/ml rRNasin RNase Inhibitor (Promega). The lysate was incubated on ice for 5 minutes. Protein A and protein G Sepharose 4 Fast Flow (GE Healthcare Life Sciences) beads were pre-swollen in NT2 buffer (50 mM Tris-HCl (pH 7.4), 150 mM NaCl, 1 mM MgCl2, 0.05% NP40) supplemented with 5% BSA to a final ratio of 1:5 for at least 1 h at 4 °C. Antibody anti-GFP (Roche) was added to the bead slurry and incubated overnight, tumbling end over end at 4 °C. Antibody-coated beads were washed with 1 ml of ice-cold NT2 buffer 4 times. After the final wash, beads were resuspended in 1 ml of ice-cold NT2 buffer and 200 units of rRNasin RNAse inhibitor were added. Lysates were centrifuged at 15,000g for 15 min to clear from large particles. The cleared lysate (2mg for endogenous miR-223, 1mg for miR-223 overexpressing cells) was added to the antibody mixture and incubated for 4 h at 4 °C tumbling end over end. Beads were then washed twice

with each of the following wash buffer: low salt wash buffer (20mM Tris HCl pH 8.0, 150mM NaCl, 0.1% SDS, 1% triton X-100 and 2mM EDTA), high salt wash buffer (20mM Tris HCl pH 8.0, 500mM NaCl, 0.1% SDS, 1% triton X-100 and 2mM EDTA) and NT2 buffer supplemented with 2M Urea and 1% sodium deoxycholate. Beads were then resuspended in 1 ml of NT2 buffer and 400 µl were saved for Western blotting analysis after the addition of 3x laemmli buffer. The remaining 600 µl were used for qRT-PCR analysis: beads were pelletted down and resuspended in 50 µl of NT2 buffer supplemented with 30 µg of proteinase K. The mixture was incubated at 55°C for 30 min and Trizol reagent was then added to isolate the RNA from the immunoprecipitated pellet. The extracted RNA was retrotranscribed using the TaqMan MicroRNA Reverse Transcription Kit and analyzed by qRT-PCR using TaqMan MicroRNA Assays, as described before. The PCR products were also separated on a 15% non denaturing-polyacrylamide gel.

Preparation of protein lysates and immunoblotting

3T3 p27KO fibroblasts overexpressing p27 (p27WT, p27CK$^-$, p27KR) were grown in DMEM with 10% FBS and harvested at exponential growth.

MDA-MB-231, HT1080 cell lines overexpressing miR-223 were transfected with p27 expression vectors using FuGENE HD transfection reagent (Promega), as described above and 48 hours later cells were harvested.

p27WT and p27KO MEFs were harvested at EG, HC, ST, HC+ST, ST and released in complete medium (10% FBS) for indicated time. Mammary cell lines (MDA-MB-231, BT-474, HBL-100, SK-BR-3, MCF-7, T47-D, MCF-10A) were harvested at EG or HC.

To extract total proteins, cells were scraped on ice using cold RIPA lysis buffer (150mM NaCl, 50mM Tris HCl pH 8.0, 1% NP40, 0.5% sodium deoxycholate, 0.1% SDS) or NP40 lysis buffer (0.5% NP40; 50 mM HEPES pH 7; 250 mM NaCl; 5 mM EDTA; 0.5 mM EGTA, pH 8) plus a protease inhibitor cocktail (Complete™, Roche) and supplemented with 1 mM Na3VO4 (SIGMA), 10 mM NaF (SIGMA) and 1 mM DTT (SIGMA).

For immunoblotting analysis, proteins were separated in 4-20% SDS-PAGE (Criterion Precast Gel, Biorad) and transferred to nitrocellulose membranes (GE Healthcare Life Sciences). Membranes were blocked with 5% dried milk in TBS-0.1% Tween20 or in Odyssey Blocking Buffer (Licor, Biosciences) and incubated at 4°C overnight with primary antibodies. Then, membranes were incubated 1 hour at RT with horseradish peroxidase-conjugated secondary antibody (GE Healthcare Life Sciences) for ECL detection (GE

Healthcare Life Sciences) or with IR-conjugated (Alexa Fluor 680, Invitrogen or IRDye 800, Rockland) secondary antibodies for infrared detection (Odyssey Infrared Detection System, Licor). For IPs, anti-Rabbit IgG and anti-Mouse IgG True Blot (eBioscience) secondary HRP-conjugated antibodies were used.

Primary antibody were purchased from BD Biosciences: p27; from Santa Cruz: p27 (SC-C19), E2F1 (SC-193), vinculin (SC-7694); phospho-p27 (T157) (AF1555) from R&D Systems; from Roche: GFP (11814460001).

TCGA statistical analyses

We downloaded clinical, miR expression and Reverse Phase Protein Array (RPPA) data from TCGA (The Cancer Genome Atlas) available through the associated files of the paper Comprehensive molecular portraits of human breast tumors, Nature, September 27, 2012 https://tcga-data.nci.nih.gov/docs/publications/brca_2012/ (166).

Statistical analyses were performed in R (version 2.14.2) (http:///www.r-project.org/). All tests were two-sided and considered statistical significant at the 0.05 level. The Log-rank test was employed to determine the significance of the association between miR-223 (MIMAT0000280) expression and total p27, p27 T157 and p27 T198 RPPA.

The Spearman's rank-order correlation test was applied to measure the strength of the association between miR-223 expression and p27T157 RPPA levels.

The Shapiro-Wilk test was applied to determine whether data followed a normal distribution. The analysis of variance test was applied to normally distributed data, otherwise the Kruskal-Wallis test was applied to assess the association of miR/RPPA levels with breast tumor subtypes.

References

1. **Lee RC, Feinbaum RL, Ambros V.** The C. elegans heterochronic gene lin-4 encodes small RNAs with antisense complementarity to lin-14. Cell. 1993 Dec 3;75(5):843-54.
2. **Wightman B, Ha I, Ruvkun G.** Posttranscriptional regulation of the heterochronic gene lin-14 by lin-4 mediates temporal pattern formation in C. elegans. Cell. 1993 Dec 3;75(5):855-62.
3. **Reinhart BJ, Slack FJ, Basson M. et al.** The 21-nucleotide let-7 RNA regulates developmental timing in Caenorhabditis elegans. Nature. 2000 Feb 24;403(6772):901-6.
4. **Inui M, Martello G, Piccolo S.** MicroRNA control of signal transduction. Nat Rev Mol Cell Biol. 2010 Apr;11(4):252-63.
5. **Winter J, Jung S, Keller S, et al.** Many roads to maturity: microRNA biogenesis pathways and their regulation. Nat Cell Biol. 2009 Mar;11(3):228-34.
6. **Krol J, Loedige I, Filipowicz W.** The widespread regulation of microRNA biogenesis, function and decay. Nat Rev Genet. 2010 Sep;11(9):597-610.
7. **Bartel DP**. MicroRNAs: target recognition and regulatory functions. Cell. 2009 Jan 23;136(2):215-33.
8. **Djuranovic S, Nahvi A, Green R.** A parsimonious model for gene regulation by miRNAs. Science. 2011 Feb 4;331(6017):550-3.
9. **O'Donnell KA, Wentzel EA, Zeller KI**, **et al.** c-Myc-regulated microRNAs modulate E2F1 expression. Nature. 2005 Jun 9;435(7043):839-43
10. **Ma L, Young J, Prabhala H, et al.** miR-9, a MYC/MYCN-activated microRNA, regulates E-cadherin and cancer metastasis. Nat Cell Biol. 2010 Mar;12(3):247-56.
11. **Chang TC, Yu D, Lee YS, et al.** Widespread microRNA repression by Myc contributes to tumorigenesis. Nat Genet. 2008 Jan;40(1):43-50.
12. **Viswanathan SR, Daley GQ**. Lin28: A microRNA regulator with a macro role. Cell. 2010 Feb 19;140(4):445-9.
13. **Guil S, Cáceres JF.** The multifunctional RNA-binding protein hnRNP A1 is required for processing of miR-18a. Nat Struct Mol Biol. 2007 Jul;14(7):591-6.
14. **Yates LA, Norbury CJ, Gilbert RJ.** The long and short of microRNA. Cell. 2013 Apr 25;153(3):516-9.
15. **Heo I, Ha M, Lim J, Yoon MJ, et al**. Mono-uridylation of pre-microRNA as a key step in the biogenesis of group II let-7 microRNAs. Cell. 2012 Oct 26;151(3):521-32.
16. **Lee HY, Doudna JA**. TRBP alters human precursor microRNA processing in vitro. RNA. 2012 Nov;18(11):2012-9.
17. **Fukunaga R, Han BW, Hung JH, et al.** Dicer partner proteins tune the length of mature miRNAs in flies and mammals. Cell. 2012 Oct 26;151(3):533-46.
18. **Baccarini A, Chauhan H, Gardner TJ, et al**. Kinetic analysis reveals the fate of a microRNA following target regulation in mammalian cells. Curr Biol. 2011;21:369-76.
19. **Gantier MP, McCoy CE, Rusinova I, et al.** Analysis of microRNA turnover in mammalian cells following Dicer1 ablation. Nucleic Acids Res. 2011;39:5692-03.
20. **Jung M, Schaefer A, Steiner I, et al**. Robust microRNA stability in degraded RNA preparations from human tissue and cell samples. Clin Chem. 2010 Jun;56(6):998-1006.

21. **Burroughs AM, Ando Y, de Hoon MJ, et al.** A comprehensive survey of 3' animal miRNA modification events and a possible role for 3' adenylation in modulating miRNA targeting effectiveness. Genome Res. 2010 Oct;20(10):1398-410.
22. **Bail S, Swerdel M, Liu H, et al**. Differential regulation of microRNA stability. RNA. 2010 May;16(5):1032-9.
23. **Winter J, Diederichs S**. Argonaute proteins regulate microRNA stability: Increased microRNA abundance by Argonaute proteins is due to microRNA stabilization. RNA Biol. 2011 Nov-Dec;8(6):1149-57.
24. **Tahbaz N, Carmichael JB, Hobman TC**. GERp95 belongs to a family of signal-transducing proteins and requires Hsp90 activity for stability and Golgi localization. J Biol Chem. 2001 Nov 16;276(46):43294-9.
25. **Tahbaz N, Kolb FA, Zhang H, et al**. Characterization of the interactions between mammalian PAZ PIWI domain proteins and Dicer. EMBO Rep. 2004 Feb;5(2):189-94.
26. **Robb GB, Brown KM, Khurana J, Rana TM**. Specific and potent RNAi in the nucleus of human cells. Nat Struct Mol Biol. 2005 Feb;12(2):133-7.
27. **Meister G, Landthaler M, Patkaniowska A, et al.** Human Argonaute2 mediates RNA cleavage targeted by miRNAs and siRNAs. Mol Cell. 2004 Jul 23;15(2):185-97.
28. **Calin GA, Dumitru CD, Shimizu M, et al**. Frequent deletions and downregulation of micro-RNA genes miR15 and miR16 at 13q14 in chronic lymphocytic leukemia. Proc Natl Acad Sci U S A. 2002 Nov 26;99(24):15524-9.
29. **Croce CM**. Causes and consequences of microRNA dysregulation in cancer. Nat Rev Genet. 2009 Oct;10(10):704-14.
30. **Lu J, Getz G, Miska EA, et al.** MicroRNA expression profiles classify human cancers. Nature. 2005 Jun 9;435(7043):834-8.
31. **Munker R, Calin GA**. MicroRNA profiling in cancer. Clin Sci (Lond). 2011 Aug;121(4):141-58.
32. **Volinia S, Calin GA, Liu CG, et al**. MicroRNA expression signature of human solid tumors defines cancer gene targets. Proc Natl Acad Sci U S A. 2006 Feb 14;103(7):2257-61.
33. **Calin GA, Croce CM**. MicroRNA signatures in human cancers. Nat Rev Cancer. 2006 Nov;6(11):857-66.
34. **Garzon R, Fabbri M, Cimmino A, et al**. MicroRNA expression and function in cancer. Trends Mol Med. 2006 Dec;12(12):580-7.
35. **Murakami Y, Yasuda T, Saigo K, et al**. Comprehensive analysis of microRNA expression patterns in hepatocellular carcinoma and non-tumorous tissues. Oncogene. 2006 Apr 20;25(17):2537-45.
36. **Yanaihara N, Caplen N, Bowman E, et al.** Unique microRNA molecular profiles in lung cancer diagnosis and prognosis. Cancer Cell. 2006 Mar;9(3):189-98.
37. **Weber B, Stresemann C, Brueckner B, et al**. Methylation of human microRNA genes in normal and neoplastic cells. Cell Cycle. 2007 May 2;6(9):1001-5.
38. **Brueckner B, Stresemann C, Kuner R, et al**. The human let-7a-3 locus contains an epigenetically regulated microRNA gene with oncogenic function. Cancer Res. 2007 Feb 15;67(4):1419-23.

39. **Iorio MV, Visone R, Di Leva G, et al**. MicroRNA signatures in human ovarian cancer. Cancer Res. 2007 Sep 15;67(18):8699-707.
40. **Jansson MD, Lund AH**. MicroRNA and cancer. Mol Oncol. 2012 Dec;6(6):590-610.
41. **Bui TV, Mendell JT**. Myc: Maestro of MicroRNAs. Genes Cancer. 2010 Jun 1;1(6):568-575.
42. **Kent OA, Chivukula RR, Mullendore M, et al**. Repression of the miR-143/145 cluster by oncogenic Ras initiates a tumor-promoting feed-forward pathway. Genes Dev. 2010 Dec 15;24(24):2754-9.
43. **Burk U, Schubert J, Wellner U, et al**. A reciprocal repression between ZEB1 and members of the miR-200 family promotes EMT and invasion in cancer cells. EMBO Rep. 2008 Jun;9(6):582-9.
44. **Chang TC, Wentzel EA, Kent OA, et al**. Transactivation of miR-34a by p53 broadly influences gene expression and promotes apoptosis. Mol Cell. 2007 Jun 8;26(5):745-52.
45. **He L, He X, Lim LP, et al**. A microRNA component of the p53 tumour suppressor network. Nature. 2007 Jun 28;447(7148):1130-4.
46. **Hermeking H**. MicroRNAs in the p53 network: micromanagement of tumour suppression. Nat Rev Cancer. 2012 Sep;12(9):613-26.
47. **Rüegger S, Großhans H**. MicroRNA turnover: when, how, and why. Trends Biochem Sci. 2012;37:436-46.
48. **Rissland OS, Hong SJ, Bartel DP**. MicroRNA destabilization enables dynamic regulation of the miR-16 family in response to cell-cycle changes. Mol Cell. 2011;43:993-1004.
49. **Avraham R, Sas-Chen A, Manor O, et al**. EGF decreases the abundance of microRNAs that restrain oncogenic transcription factors. Sci Signal. 2010; 3:ra43**.**
50. **Le Sage C, Nagel R, Egan DA, et al**. Regulation of the p27(Kip1) tumor suppressor by miR-221 and miR-222 promotes cancer cell proliferation. EMBO J. 2007;26:3699-708.
51. **Petrocca F, Visone R, Onelli MR, et al**. E2F1-regulated microRNAs impair TGFbeta-dependent cell-cycle arrest and apoptosis in gastric cancer. Cancer Cell 2008;13:272-86.
52. **Qin X, Wang X, Wang Y, et al**. MicroRNA-19a mediates the suppressive effect of laminar flow on cyclin D1 expression in human umbilical vein endothelial cells. Proc Natl Acad Sci U S A. 2010;107:3240-44.
53. **Bueno MJ, Malumbres M**. MicroRNAs and the cell cycle. Biochim Biophys Acta 2011;1812:592-601.
54. **Bueno MJ, Gómez de Cedrón M, Laresgoiti U, et al.** Multiple E2F-induced microRNAs prevent replicative stress in response to mitogenic signaling. Mol Cell Biol. 2010;30: 2983-95.
55. **Genovese C, Trani D, Caputi M, et al**. Cell cycle control and beyond: emerging roles for the retinoblastoma gene family. Oncogene. 2006 Aug 28;25(38):5201-9.
56. **Henley SA, Dick FA**. The retinoblastoma family of proteins and their regulatory functions in the mammalian cell division cycle. Cell Div. 2012 Mar 14;7(1):10.
57. **Garofalo M, Quintavalle C, Romano G, et al**. miR221/222 in cancer: their role in tumor progression and response to therapy. Curr Mol Med 2012;12:27-33.

58. **Grimmler M, Wang Y, Mund T, et al**. Cdk inhibitory activity and stability of p27Kip1 are directly regulated by oncogenic tyrosine kinases. Cell 2007;128:269-80.
59. **Coats S, Flanagan WM, Nourse J, et al**. Requirement of p27Kip1 for restriction point control of the fibroblast cell cycle. Science 1996;272:877-80.
60. **Galardi S, Mercatelli N, Giorda E, et al**. miR-221 and miR-222 expression affects the proliferation potential of human prostate carcinoma cell lines by targeting p27Kip1. J Biol Chem. 2007 Aug 10;282(32):23716-24.
61. **Sun M, Liu XH, Li JH, et al**. MiR-196a is upregulated in gastric cancer and promotes cell proliferation by downregulating p27(kip1). Mol Cancer Ther. 2012 Apr;11(4):842-52.
62. **Guo SL, Peng Z, Yang X, et al**. miR-148a promoted cell proliferation by targeting p27 in gastric cancer cells. Int J Biol Sci. 2011 May 5;7(5):567-74.
63. **Cuesta R, Martínez-Sánchez A, Gebauer F**. miR-181a regulates cap-dependent translation of p27(kip1) mRNA in myeloid cells. Mol Cell Biol. 2009 May;29(10):2841-51.
64. **Coller HA, Sang L, Roberts JM**: A new description of cellular quiescence. PLoS Biology. 2006, 4:e83.
65. **Iyer VR, Eisen MB, Ross DT, et al**. The transcriptional program in the response of human fibroblasts to serum. Science. 1999, 283:83-87.
66. **Liu H, Adler AS, Segal E, et al**. A transcriptional program mediating entry into cellular quiescence. PLoS Genet. 2007, 3:e91.
67. **Schneider C, King RM, Philipson L**. Genes specifically expressed at growth arrest of mammalian cells. Cell. 1988, 54:787-793.
68. **Polyak K, Kato JY, Solomon MJ, et al.** p27Kip1, a cyclin-Cdk inhibitor, links transforming growth factor-beta and contact inhibition to cell cycle arrest. Genes Dev. 1994;8:9-22
69. **Bartel DP**. MicroRNAs: genomics, biogenesis, mechanism, and function. Cell. 2004, 116:281-297.
70. **Tsuchiya N, Ochiai M, Nakashima K, et al**. SND1, a component of RNA-induced silencing complex, is up-regulated in human colon cancers and implicated in early stage colon carcinogenesis. Cancer Res. 2007 Oct 1;67(19):9568-76.
71. **Suh EJ, Remillard MY, Legesse-Miller A, et al**. A microRNA network regulates proliferative timing and extracellular matrix synthesis during cellular quiescence in fibroblasts. Genome Biol. 2012 Dec 22;13(12):R121.
72. **Hwang HW, Wentzel EA, Mendell JT**. Cell-cell contact globally activates microRNA biogenesis. Proc Natl Acad Sci U S A. 2009 Apr 28;106(17):7016-21.
73. **Bertero T, Gastaldi C, Bourget-Ponzio I, et al**. CDC25A targeting by miR-483-3p decreases CCND-CDK4/6 assembly and contributes to cell cycle arrest. Cell Death Differ. 2013 Jun;20(6):800-11.
74. **Jurmeister S, Baumann M, Balwierz A, et al**. MicroRNA-200c represses migration and invasion of breast cancer cells by targeting actin-regulatory proteins FHOD1 and PPM1F. Mol Cell Biol. 2012 Feb;32(3):633-51.
75. **Chen CZ, Lodish HF.** MicroRNAs as regulators of mammalian hematopoiesis. Semin Immunol. 2005 Apr;17(2):155-65.

76. **Chen CZ, Li L, Lodish HF, et al.** MicroRNAs modulate hematopoietic lineage differentiation. Science. 2004 Jan 2;303(5654):83-6.
77. **Fukao T, Fukuda Y, Kiga K, et al.** An evolutionarily conserved mechanism for microRNA-223 expression revealed by microRNA gene profiling. Cell. 2007 May 4;129(3):617-31.
78. **Fazi F, Racanicchi S, Zardo G, et al**. Epigenetic silencing of the myelopoiesis regulator microRNA-223 by the AML1/ETO oncoprotein. Cancer Cell. 2007 Nov;12(5):457-66.
79. **Zhou K, Yi S, Yu Z, et al**. MicroRNA-223 expression is uniformly down-regulated in B cell lymphoproliferative disorders and is associated with poor survival in patients with chronic lymphocytic leukemia. Leuk Lymphoma. 2012 Jun;53(6):1155-61.
80. **Stamatopoulos B, Meuleman N, Haibe-Kains B, et al**. microRNA-29c and microRNA-223 down-regulation has in vivo significance in chronic lymphocytic leukemia and improves disease risk stratification. Blood. 2009 May 21;113(21):5237-45.
81. **Pulikkan JA, Dengler V, Peramangalam PS, et al**. Cell-cycle regulator E2F1 and microRNA-223 comprise an autoregulatory negative feedback loop in acute myeloid leukemia. Blood. 2010 Mar 4;115(9):1768-78.
82. **Gusscott S, Kuchenbauer F, Humphries RK, et al**. Notch-mediated repression of miR-223 contributes to IGF1R regulation in T-ALL. Leuk Res. 2012 Jul;36(7):905-11.
83. **Johnnidis JB, Harris MH, Wheeler RT, et al**. Regulation of progenitor cell proliferation and granulocyte function by microRNA-223. Nature. 2008 Feb 28;451(7182):1125-9.
84. **Wong QW, Lung RW, Law PT, et al.** MicroRNA-223 is commonly repressed in hepatocellular carcinoma and potentiates expression of Stathmin1. Gastroenterology. 2008 Jul;135(1):257 69.
85. **Li S, Li Z, Guo F, et al**. miR-223 regulates migration and invasion by targeting Artemin in human esophageal carcinoma. J Biomed Sci. 2011 Mar 31;18:24.
86. **Li G, Cai M, Fu D, et al**. Heat shock protein 90B1 plays an oncogenic role and is a target of microRNA-223 in human osteosarcoma. Cell Physiol Biochem. 2012;30(6):1481-90.
87. **Glasgow SM, Laug D, Brawley VS, et al.** The miR-223/nuclear factor I-A axis regulates glial precursor proliferation and tumorigenesis in the CNS. J Neurosci. 2013 Aug 14;33(33):13560-8.
88. **Li J, Guo Y, Liang X, et al**. MicroRNA-223 functions as an oncogene in human gastric cancer by targeting FBXW7/hCdc4. J Cancer Res Clin Oncol. 2012 May;138(5):763-74.
89. **Li X, Zhang Y, Zhang H, et al**. miRNA-223 promotes gastric cancer invasion and metastasis by targeting tumor suppressor EPB41L3. Mol Cancer Res. 2011 Jul;9(7):824-33.
90. **Xu J, Wu C, Che X, et al**. Circulating microRNAs, miR-21, miR-122, and miR-223, in patients with hepatocellular carcinoma or chronic hepatitis. Mol Carcinog. 2011 Feb;50(2):136-42.
91. **Zeng X, Xiang J, Wu M, et al**. Circulating miR-17, miR-20a, miR-29c, and miR-223 combined as non-invasive biomarkers in nasopharyngeal carcinoma. PLoS One. 2012;7(10):e46367.

92. **Yang M, Chen J, Su F, et al**. Microvesicles secreted by macrophages shuttle invasion-potentiating microRNAs into breast cancer cells. Mol Cancer. 2011 Sep 22;10:117.
93. **Nurse P**. A long twentieth century of the cell cycle and beyond. Cell. 2000 Jan 7;100(1):71-8.
94. **Heichman KA**, **Roberts JM.** Rules to replicate by. Cell. 1994 Nov 18;79(4):557-62.
95. **Wuarin J and Nurse P**. Regulating S-phase: CDKs, licensing and proteolysis. Cell. 1996 Jun 14;85(6):785-7.
96. **Hunt T**. Cell biology. Cell cycle gets more cyclins. Nature. 1991 Apr 11;350(6318):462 3.
97. **Sherr CJ**. G1 phase progression: cycling on cue. Cell. 1994 Nov 18;79(4):551-5.
98. **Sherr CJ**. Growth factor-regulated G1 cyclins. Stem Cells. 1994. 12 Suppl 1:47-55; discussion 55-7.
99. **Matsushime H**, **Roussel MF, Ashmun RA**, **et al.** Colony-stimulating factor 1 regulates novel cyclins during the G1 phase of the cell cycle. Cell. 1991 May 17;65(4):701-13.
100. **Xiong Y**, **Connolly T, Futcher B, et al**. Human D-type cyclin. Cell. 1991 May 17;65(4):691-9.
101. **Matsushime H**, **Ewen ME, Strom DK, et al**. Identification and properties of an atypical catalytic subunit (p34PSK-J3/cdk4) for mammalian D type G1 cyclins. Cell. 1992 Oct 16;71(2):323-34.
102. **Meyerson M**, **Harlow E**. Identification of G1 kinase activity for cdk6, a novel cyclin D partner. Mol Cell Biol. 1994 Mar;14(3):2077-86.
103. **Ewen ME**, **Sluss HK, Sherr CJ, et al.** Functional interactions of the retinoblastoma protein with mammalian D-type cyclins. Cell. 1993 May 7;73(3):487-97.
104. **Kato J**, **Matsushime H, Hiebert SW, et al.** Direct binding of cyclin D to the retinoblastoma gene product (pRb) and pRb phosphorylation by the cyclin D-dependent kinase CDK4. Genes Dev. 1993 Mar;7(3):331-42.
105. **Nevins JR**. Toward an understanding of the functional complexity of the E2F and retinoblastoma families. Cell Growth Differ. 1998 Aug;9(8):585-93.
106. **Koff A**, **Giordano A, Desai D, et al**. Formation and activation of a cyclin E-cdk2 complex during the G1 phase of the human cell cycle. Science. 1992 Sep 18;257(5077):1689-94.
107. **Koff A**, **Cross F, Fisher A, et al.** Human cyclin E, a new cyclin that interacts with two members of the CDC2 gene family. Cell. 1991Sep 20;66(6):1217-28.
108. **Lew DJ, Dulić V, Reed SI**. Isolation of three novel human cyclins by rescue of G1 cyclin (Cln) function in yeast. Cell. 1991 Sep 20;66(6):1197-206.
109. **Dulić V**, **Lees E, Reed SI**. Association of human cyclin E with a periodic G1-S-phase protein kinase. Science. 1992 Sep 25;257(5078):1958-61.
110. **Hinds PW**, **Mittnacht S, Dulic V, et al**. Regulation of retinoblastoma protein functions by ectopic expression of human cyclins. Cell 1992. Sep 18;70(6):993-1006.
111. **Kelly BL**, **Wolfe KG, Roberts JM**. Identification of a substrate-targeting domain in cyclin E necessary for phosphorylation of the retinoblastoma protein. Proc Natl Acad Sci U S A. 1998 Mar 3;95(5):2535-40.

112. **Lundberg AS**, **Weinberg RA**. Functional inactivation of the retinoblastoma protein requires sequential modification by at least two distinct cyclin-cdk complexes. Mol Cell Biol. 1998 Feb;18(2):753-61.
113. **Pines J**. Four-dimensional control of the cell cycle. Nat Cell Biol. 1999 Jul;1(3):E73-9.
114. **Belletti B**, **Nicoloso MS, Schiappacassi M, et al**. p27(kip1) functional regulation in human cancer: a potential target for therapeutic designs. Curr Med Chem. 2005;12(14):1589-605.
115. **Hannon GJ**, **Beach D**. p15INK4B is a potential effector of TGF-beta-induced cell cycle arrest. Nature. 1994 Sep 15;371(6494):257-61.
116. **Serrano M**, **Hannon GJ, Beach D**. A new regulatory motif in cell-cycle control causing specific inhibition of cyclin D/CDK4. Nature. 1993 Dec 16;366(6456):704-7.
117. **Guan KL**, **Jenkins CW, Li Y, et al.** Growth suppression by p18, a p16INK4/MTS1- and p14INK4B/MTS2-related CDK6 inhibitor, correlates with wild type pRb function. Genes Dev. 1994 Dec 15;8(24):2939-52.
118. **Hirai H**, **Roussel MF, Kato JY, et al.** Novel INK4 proteins, p19 and p18, are specific inhibitors of the cyclin D-dependent kinases CDK4 and CDK6. Mol Cell Biol. 1995 May;15(5):2672-81.
119. **Chan FK**, **Zhang J, Cheng L, et al**. Identification of human and mouse p19, a novel CDK4 and CDK6 inhibitor with homology to p16ink4. Mol Cell Biol. 1995 May;15(5):2682-8.
120. **Harper JW**, **Adami GR, Wei N, et al.** The p21 Cdk-interacting protein Cip1 is a potent inhibitor of G1 cyclin-dependent kinases. Cell. 1993 Nov 19;75(4):805-16.
121. **Noda A**, **Ning Y, Venable SF, et al**. Cloning of senescent cell-derived inhibitors of DNA synthesis using an expression screen. Exp Cell Res. 1994 Mar;211(1):90-8.
122. **Xiong Y**, **Hannon GJ, Zhang H, et al**. p21 is a universal inhibitor of cyclin kinases. Nature. 1993 Dec 16;366(6456):701-4.
123. **Toyoshima H**, **Hunter T.** p27, a novel inhibitor of G1 cyclin-Cdk protein kinase activity, is related to p21. Cell. 1994 Jul 15;78(1):67-74.
124. **Lee MH, Reynisdóttir I, Massagué J**. Cloning of p57KIP2, a cyclin-dependent kinase inhibitor with unique domain structure and tissue distribution. Genes Dev. 1995 Mar 15;9(6):639-49.
125. **Matsuoka S**, **Edwards MC, Bai C, et al**. p57KIP2, a structurally distinct member of the p21CIP1 Cdk inhibitor family, is a candidate tumor suppressor gene. Genes Dev. 1995 Mar 15;9(6):650-62.
126. **Matsuoka S**, **Thompson JS, Edwards MC, et al.** Imprinting of the gene encoding a human cyclin-dependent kinase inhibitor, p57KIP2, on chromosome 11p15. Proc Natl Acad Sci U S A. 1996 Apr 2;93(7):3026-30.
127. **Elledge SJ**, **Winston J, Harper JW**. A question of balance: the role of cyclin-kinase inhibitors in development and tumorigenesis. Trends Cell Biol. 1996 Oct;6(10):388-92.
128. 128 **Koff A**, **Ohtsuki M, Polyak K, et al.** Negative regulation of G1 in mammalian cells: inhibition of cyclin E-dependent kinase by TGF-beta. Science. 1993 Apr 23;260(5107):536-9.

129. **Chen J, Jackson PK, Kirschner MW, et al.** Separate domains of p21 involved in the inhibition of Cdk kinase and PCNA. Nature. 1995 Mar 23;374(6520):386-8.
130. **Chen J**, **Saha P, Kornbluth S, et al.** Cyclin-binding motifs are essential for the function of p21CIP1. Mol Cell Biol. 1996 Sep;16(9):4673-82.
131. **Nakanishi M**, **Robetorye RS, Adami GR, et al.** Identification of the active region of the DNA synthesis inhibitory gene p21Sdi1/CIP1/WAF1. EMBO J. 1995 Feb 1;14(3):555-63.
132. **Fagotto F, Gumbiner BM.** Cell contact-dependent signaling. Dev Biol. 1996 Dec 15;180(2):445-54.
133. **Abercrombie M**. Contact inhibition and malignancy. Nature 1979;281:259–62.
134. **Dietrich C, Wallenfang K, Oesch F, et al.** Differences in the mechanisms of growth control in contact-inhibited and serum-deprived human fibroblasts. Oncogene. 1997 Nov 27;15(22):2743-7.
135. **Holley RW, Armour R, Baldwin JH**. Density-dependent regulation of growth of BSC-1 cells in cell culture: growth inhibitors formed by the cells. Proc Natl Acad Sci U S A. 1978 Apr;75(4):1864-6.
136. **Hanahan D, Weinberg RA**. The hallmarks of cancer. Cell. 2000 Jan 7;100(1):57-70.
137. **McClatchey AI, Yap AS**. Contact inhibition (of proliferation) redux. Curr Opin Cell Biol. 2012 Oct;24(5):685-94.
138. **Aoki J, Umeda M, Takio K, et al.** Neural cell adhesion molecule mediates contact-dependent inhibition of growth of near-diploid mouse fibroblast cell line m5S/1M. J Cell Biol. 1991 Dec;115(6):1751-61.
139. **Takahashi K, Suzuki K.** Density-dependent inhibition of growth involves prevention of EGF receptor activation by E-cadherin-mediated cell-cell adhesion. Exp Cell Res. 1996 Jul 10;226(1):214-22.
140. **Kandikonda S, Oda D, Niederman R, et al.** Cadherin-mediated adhesion is required for normal growth regulation of human gingival epithelial cells. Cell Adhes Commun. 1996 Jul;4(1):13-24.
141. **Levenberg S, Yarden A, Kam Z, et al**. p27 is involved in N-cadherin-mediated contact inhibition of cell growth and S-phase entry. Oncogene. 1999 Jan 28;18(4):869-76.
142. **St Croix B, Sheehan C, Rak JW, et al.** E-Cadherin-dependent growth suppression is mediated by the cyclin-dependent kinase inhibitor p27(KIP1). J Cell Biol. 1998 Jul 27;142(2):557-71.
143. **Motti ML, Califano D, Baldassarre G, et al**. Reduced E-cadherin expression contributes to the loss of p27kip1-mediated mechanism of contact inhibition in thyroid anaplastic carcinomas. Carcinogenesis. 2005 Jun;26(6):1021-34
144. **Todaro GJ, Green H.** Quantitative studies of the growth of mouse embryo cells in culture and their development into established lines. J Cell Biol. 1963 May;17:299-313.
145. **Holley RW, Kiernan JA.**"Contact inhibition" of cell division in 3T3 cells. Proc Natl Acad Sci U S A. 1968 May;60(1):300-4.
146. **Vogel A, Ross R, Raines E.** Role of serum components in density-dependent inhibition of growth of cells in culture. Platelet-derived growth factor is the major serum determinant of saturation density. J Cell Biol. 1980 May;85(2):377-85.

147. **Brown KD, Yeh YC, Holley RW.** Binding, internalization, and degradation of epidermal growth factor by balb 3T3 and BP3T3 cells: relationship to cell density and the stimulation of cell proliferation. J Cell Physiol. 1979 Aug;100(2):227-38.
148. **Pagano M**, **Tam SW, Theodoras AM, et al.** Role of the ubiquitin-proteasome pathway in regulating abundance of the cyclin-dependent kinase inhibitor p27. Science. 1995 Aug 4;269(5224):682-5.
149. **Montagnoli A**, **Fiore F, Eytan E, et al.** Ubiquitination of p27 is regulated by Cdk-dependent phosphorylation and trimeric complex formation. Genes Dev. 1999 May 1;13(9):1181-9.
150. **Nguyen H**, **Gitig DM, Koff A.** Cell-free degradation of p27(kip1), a G1 cyclin-dependent kinase inhibitor, is dependent on CDK2 activity and the proteasome. *Mol* Cell Biol. 1999 Feb;19(2):1190-201.
151. **Hengst L, Reed SI.** Inhibitors of the Cip/Kip family. Curr Top Microbiol Immunol. 1998;227:25-41.
152. **Kato A, Takahashi H, Takahashi Y, et al.** Contact inhibition-induced inactivation of the cyclin D-dependent kinase in rat fibroblast cell line, 3Y1. Leukemia. 1997 Apr;11 Suppl 3:361-2.
153. **Zhang X, Wharton W, Donovan M, et al.** Density-dependent growth inhibition of fibroblasts ectopically expressing p27(kip1). Mol Biol Cell. 2000 Jun;11(6):2117-30.
154. **Kim TY, Kim WI, Smith RE, et al.** Differential activity of TGF-beta2 on the expression of p27Kip1 and Cdk4 in actively cycling and contact inhibited rabbit corneal endothelial cells. Mol Vis. 2001 Nov 20;7:261-70.
155. **Fuse T, Tanikawa M, Nakanishi M, et al.** p27Kip1 expression by contact inhibition as a prognostic index of human glioma. J Neurochem. 2000 Apr;74(4):1393-9.
156. **Nakatsuji Y, Miller RH.** Density dependent modulation of cell cycle protein expression in astrocytes. J Neurosci Res. 2001 Nov 1;66(3):487-96.
157. **Hirano M, Kanaide H, Hirano K.** Rac1-dependent transcriptional up-regulation of p27Kip1 by homophilic cell-cell contact in vascular endothelial cells. Biochim Biophys Acta. 2007 Oct;1773(10):1500-10.
158. **Lwin T, Hazlehurst LA, Dessureault S, et al.** Cell adhesion induces p27Kip1-associated cell-cycle arrest through down-regulation of the SCFSkp2 ubiquitin ligase pathway in mantle-cell and other non-Hodgkin B-cell lymphomas. Blood. 2007 Sep 1;110(5):1631-8. Epub 2007 May 14.
159. **Lee Y, Kim M, Han J, et al**. MicroRNA genes are transcribed by RNA polymerase II. EMBO J. 2004;13: 4051-60.
160. **Nevins JR**. The Rb/E2F pathway and cancer. Hum Mol Genet 2001;10:699-703.
161. **Fero ML, Rivkin M, Tasch M, et al**. A syndrome of multiorgan hyperplasia with features of gigantism, tumorigenesis, and female sterility in p27(Kip1)-deficient mice. Cell 1996;85:733-44.
162. **Martín A, Odajima J, Hunt SL, et al**. Cdk2 is dispensable for cell cycle inhibition and tumor suppression mediated by p27(Kip1) and p21(Cip1). Cancer Cell 2005;7:591-98.
163. **Schiappacassi M, Lovisa S, Lovat F, et al.** Role of T198 modification in the regulation of p27(Kip1) protein stability and function. PLoS One. 2011, e17673.

164. **Wu FY, Wang SE, Sanders ME, et al.** Reduction of cytosolic p27(Kip1) inhibits cancer cell motility, survival, and tumorigenicity. Cancer Res. 2006;66:2162-72.
165. **Belletti B, Baldassarre G.** New light on p27(kip1) in breast cancer. Cell Cycle 2012;11:3701-02.
166. **Cancer Genome Atlas Network**. Comprehensive molecular portraits of human breast tumours. Nature. 2012;490:61-70.
167. **Liang J, Zubovitz J, Petrocelli T, et al**. PKB/Akt phosphorylates p27, impairs nuclear import of p27 and opposes p27-mediated G1 arrest. Nat Med. 2002;8:1153-60.
168. **Takeshita F, Patrawala L, Osaki M, et al**. Systemic delivery of synthetic microRNA-16 inhibits the growth of metastatic prostate tumors via downregulation of multiple cell-cycle genes. Mol Ther. 2010 Jan;18(1):181-7.
169. **Sarkar S, Dey BK, Dutta A**. MiR-322/424 and -503 are induced during muscle differentiation and promote cell cycle quiescence and differentiation by down-regulation of Cdc25A. Mol Biol Cell. 2010 Jul 1;21(13):2138-49.
170. **Johnson CD, Esquela-Kerscher A, Stefani G, et al**. The let-7 microRNA represses cell proliferation pathways in human cells. Cancer Res. 2007 Aug 15;67(16):7713-22.
171. **Benetti R, Gonzalo S, Jaco I, et al.** A mammalian microRNA cluster controls DNA methylation and telomere recombination via Rbl2-dependent regulation of DNA methyltransferases. Nat Struct Mol Biol. 2008 Mar;15(3):268-79.
172. **Perna D, Fagà G, Verrecchia A, et al.** Genome-wide mapping of Myc binding and gene regulation in serum-stimulated fibroblasts. Oncogene. 2012 Mar 29;31(13):1695-709
173. **Litovchick L, Sadasivam S, Florens L, et al.** Evolutionarily conserved multisubunit RBL2/p130 and E2F4 protein complex represses human cell cycle-dependent genes in quiescence. Mol Cell. 2007 May 25;26(4):539-51.
174. **Medina R, Zaidi SK, Liu CG, et al**. MicroRNAs 221 and 222 bypass quiescence and compromise cell survival. Cancer Res. 2008 Apr 15;68(8):2773-80.
175. **Liu N, Williams AH, Kim Y, et al.** An intragenic MEF2-dependent enhancer directs muscle-specific expression of microRNAs 1 and 133. Proc Natl Acad Sci U S A. 2007 Dec 26;104(52):20844-9.
176. **Zhao Y, Samal E, Srivastava D**. Serum response factor regulates a muscle-specific microRNA that targets Hand2 during cardiogenesis. Nature. 2005 Jul 14;436(7048):214-20
177. **Kim YK, Heo I, Kim VN**. Modifications of small RNAs and their associated proteins. Cell. 2010 Nov 24;143(5):703-9.
178. **Lee M, and Pellegata NS**. Multiple Endocrine Neoplasia Type 4. In Endocrine Tumor Syndromes and Their Genetics C.A. Stratakis, ed. (Karger) 2013, 63-78.
179. **Baldassarre G, Belletti B, Nicoloso MS, et al**. p27(Kip1)-stathmin interaction influences sarcoma cell migration and invasion. Cancer Cell. 2005;7:51-63.
180. **Lu S, Sun YH, Chiang VL**. Adenylation of plant miRNAs. Nucleic Acids Res 2009;37, 1878-85.
181. **Wang L, Brown SJ**. BindN: a web-based tool for efficient prediction of DNA and RNA binding sites in amino acid sequences. Nucleic Acids Res 2006;34: 243-48.

182. **Keene JD, Komisarow JM, Friedersdorf MB.** RIP-Chip: the isolation and identification of mRNAs, microRNAs and protein components of ribonucleoprotein complexes from cell extracts. Nat Protoc. 2006;1:302-07.

PUBLICATIONS

Contact inhibition modulates intracellular levels of miR-223 in a p27kip1-dependent manner.

Joshua Armenia, Linda Fabris, Francesca Lovat, Stefania Berton, Ilenia Segatto, Sara D'Andrea, Cristina Ivan, Luciano Cascione, George A.Calin, Carlo M.Croce, Alfonso Colombatti, Andrea Vecchione, Barbara Belletti and Gustavo Baldassarre.

Oncotarget, Advance Online Publications, March 4 2014.

p70S6 Kinase Mediates Breast Cancer Cell Survival in Response to Surgical Wound Fluid Stimulation.

Ilenia Segatto, Stefania Berton, Maura Sonego, Samuele Massarut, Linda Fabris, **Joshua Armenia**, Alfonso Colombatti, Andrea Vecchione, Gustavo Baldassarre, Barbara Belletti.

Molecular Oncology, in press doi: 10.1016/j.molonc.2014.02.006.

Inhibition of breast cancer local relapse by targeting p70S6 kinase activity.

Segatto I, Berton S, Sonego M, Massarut S, D'Andrea S, Perin T, Fabris L, **Armenia J**, Rampioni G, Lovisa S, Schiappacassi M, Colombatti A, Bristow RG, Vecchione A, Baldassarre G, Belletti B.

J Mol Cell Biol. 2013 Dec;5(6):428-31. doi: 10.1093/jmcb/mjt027. Epub 2013 Jul 29.

ACKNOWLEDGEMENTS

This work was performed in the Division of Experimental Oncology 2 at Centro di Riferimento Oncologico (CRO) of Aviano (National Cancer Institute), directed by Prof. Alfonso Colombatti.

I am grateful to SCICC lab and in particular to Dr. Barbara Belletti and Dr. Gustavo Baldassarre.